Borelli, Luan; Góes, Geraldo Sandoval

Article

The macroeconomics of epidemics: Interstate heterogeneity in Brazil

EconomiA

Provided in Cooperation with:
The Brazilian Association of Postgraduate Programs in Economics (ANPEC), Rio de Janeiro

Suggested Citation: Borelli, Luan; Góes, Geraldo Sandoval (2021) : The macroeconomics of epidemics: Interstate heterogeneity in Brazil, EconomiA, ISSN 1517-7580, Elsevier, Amsterdam, Vol. 22, Iss. 3, pp. 164-197, https://doi.org/10.1016/j.econ.2021.11.001

This Version is available at:
https://hdl.handle.net/10419/266989

EconomiA 22 (2021) 164–197

HOSTED BY

ELSEVIER

Contents lists available at ScienceDirect

EconomiA

journal homepage: www.elsevier.com/locate/econa

The macroeconomics of epidemics: Interstate heterogeneity in Brazil☆

Luan Borelli[a,b,*], Geraldo Sandoval Góes[a]

[a] Institute for Applied Economic Research (IPEA-RJ), Brazil.
[b] EPGE Brazilian School of Economics and Finance (FGV EPGE), Brazil.

ARTICLE INFO

Article history:
Received 14 July 2021
Received in revised form 28 October 2021
Accepted 8 November 2021
Available online 28 December 2021

JEL Classification:
E1
I1
H0

Keywords:
Epidemics
COVID-19
States
Recessions
Containment policy
SIR-macro model

ABSTRACT

We applied the SIR-macro model proposed by Eichenbaum et al. (2020) in its complete version to comparatively study the interaction between economic decisions and COVID-19 epidemics in five different Brazilian states: São Paulo (SP), Amazonas (AM), Ceará (CE), Rio de Janeiro (RJ), and Pernambuco (PE). Our goal was to analyze qualitatively how the main intrinsic differences of each of these states could affect the epidemic dynamics and its consequences. We computed and compared the model for each of the states, both in competitive equilibrium and under optimal containment policy adoption, and analyzed the implications of optimal policy adoption. We concluded that the intrinsic characteristics of the five different states could imply relevant differences in the general dynamics of the epidemic, in the optimal containment policies, in the effect of the adoption of these policies, and the severity of the economic recessions. One year after the original *ex-ante* calibration, we evaluated the death toll and economic recession predicted by the model comparing it against real data. The model predictions showed to be qualitatively sufficient to anticipate the size of the pandemic risk that later materialized in Brazil.

1. Introduction

As COVID-19 spread throughout Brazil, governors of the country struggled with the challenge of understanding and managing the epidemic that ravaged the states they command. When compared to other smaller countries, this challenge seemed to be even more complicated in Brazil, due to its continental geographic and demographic dimensions and the huge heterogeneity of the characteristics of its states.

Early in May 2020, a study by Hallal et al. (2020) already illustrated how this heterogeneity could affect the epidemic dynamics around the country. The study reported the first wave of seroprevalence surveys relying upon household probabilistic samples of 133 large sentinel cities in Brazil, including 25.025 participants from all 26 states and the Federal District, and found that the seroprevalence of antibodies to SARS-CoV-2, assessed using a lateral flow rapid test, varied markedly across the cities

☆ Production and hosting by National Association of Postgraduate Centers in Economics, ANPEC

* Correspondence to: Institute for Applied Economic Research (IPEA), Av. Presidente Vargas, 730, 16th floor – Towers 3 and 4, Center, Rio de Janeiro, RJ, Brazil.
E-mail address: contato@luanborelli.net (L. Borelli).

https://doi.org/10.1016/j.econ.2021.11.001

and regions, from below 1% in most cities in the South and Center-West regions to up to 25% in the city of Breves in the Amazon (North) region.

To support facing this type of challenge that required quick responses, economists promoted a significant change and adjustment in their research agendas. As put by Susskind and Vines (2020) in March 2020: "…only 6 months ago few economists knew anything about SIR models. Now we all know that the central framework for studying the spread of any infectious disease is the SIR model."

Economists began to engage in public and academic discussions about how to combat the unprecedented COVID-19 crisis, becoming professionally involved in a health crisis like never before (see Boianovsky, 2021). Researches were produced in record time, in large volume, and under very uncertain circumstances.[1]

These efforts were not limited to the international community abroad. In Brazil, research was also produced at a surprising speed despite all the limitations related to the uncertainty and the scarcity of data at the time. As raised by Boianovsky (2021), examples include the application of the SIR model for evaluating social distancing policies (e.g. Morato et al., 2020; Bastos and Cajueiro, 2020); the assessment of Covid-19's macroeconomic and sectorial impacts (e.g. Haddad et al., 2020a, 2020b; Dweck et al., 2020); the assessment of normative and health policy aspects (e.g. Rache et al., 2020; Viegas et al., 2020; Nunes et al., 2020); and the development of prediction models (e.g. Medeiros et al., 2020; Campos et al., 2021).

In this paper, we present our calibration of the SIR-macro model proposed by Eichenbaum et al. (2020). The calibration to be presented was originally made in May 2020. Differently from the epidemiology models that have been widely used to predict the course of epidemics (e.g. Ferguson et al., 2020), the SIR-macro model extends the classical SIR model (an acronym for Susceptible, Infected and Recovered) originally proposed by Kermack and McKendrick (1927) incorporating an important factor that can potentially influence the dynamics of the epidemics: the interaction between economic decisions and infection rates. In this new extended model, the people's decision to cut back on consumption and work reduces the severity of the epidemic as measured by total deaths. The same decisions exacerbate the size of the recession caused by the epidemic.

The objective of the calibration was to investigate how and how much the interstate heterogeneity could affect the dynamics of epidemics in Brazilian states. An answer to this question could provide, e.g., insights on the consequences of conducting aggregated containment policies for countries as a whole or disaggregated policies by states or regions.

We computed the model for five Brazilian states. We considered, for each of these states, two scenarios: one under competitive equilibrium (no policy adoption) and the other under optimal policy adoption. The criteria for the selection of these five states was the severity of the epidemics at the moment of the research. Thus, we selected the five Brazilian states that presented the worst epidemic situation among all the 26 Brazilian states. The selected states were São Paulo (SP), Amazonas (AM), Ceará (CE), Rio de Janeiro (RJ) and Pernambuco (PE).

The different intrinsic characteristics of these states were incorporated in the results through our calibration strategy for the parameter and variable values of the model. Our calibration allowed the results to incorporate interstate differences relative to the following aspects: i) size of the population, ii) per capita income; iii) average time devoted to work; iv) average time spent in public transport; v) average time devoted to household chores; vi) the average number of people per residence; vii) the number of workers; viii) the number of students and ix) infection fatality rates estimated with the evolution of the epidemic until the moment of the research.

We compared the differences in the epidemic dynamics and their consequences between the five states both for the competitive equilibrium scenario (without adopting containment policies) and for the scenario in which optimal containment policies are adopted. We also compared the differences in the optimal containment policies required for each state and evaluated the effects of adopting these policies on each of these states.

As a result of these analyzes, we concluded that the intrinsic characteristics of the five different states could imply relevant differences in their epidemic dynamics, in the optimal containment policies to be adopted, in the effect of adopting these policies, and in the severity of the economic recessions resulting from the epidemic.

This conclusion emphasized the importance of a disaggregated analysis of countries with huge geographic and demographic dimensions – such as Brazil – in the formulation of coordinated policies to combat COVID-19. At the time of the first draft of the paper, we warned that the adoption of single centralized and aggregated policies for huge and heterogeneous countries like Brazil could trigger a series of containment policy errors across the country's states and regions, deepening both the economic recession and the number of deaths resulting from the epidemic.

Approximately one year after the original *ex-ante* calibration, we evaluate the predictions made by the model comparing it to *ex-post* real-world data. The results of the model showed to be reasonably consistent, at least qualitatively, when considering the simplicity of the model and the context and the time when it was calibrated – surrounded by uncertainty about the nature of the virus and by the scarcity of data to calibrate the model in a more precise way. We conclude that, in times and circumstances of emergency, the model could have been used to qualitatively anticipate the potential tragedy of the pandemic that later materialized in Brazil.

[1] As Boianovsky (2021) puts it, between March and November 2020, the American NBER (National Bureau of Economic Research) alone released around 300 pandemic-related technical papers. In March 2020, the Centre for Economic Policy Research (CEPR), a European research center based in London, launched Covid Economics, Vetted and Real-Time Papers, formed by online issues of collected discussion papers made available weekly on average, according to a fast-track system. The CEPR also produced books on the subject, aimed at a broader audience. Several special issues and symposia also came out throughout 2020.

Our paper is organized as follows. In Section 2, we describe the SIR-macro model of Eichenbaum et al. (2020) in its complete version. In Section 3, we discuss our calibration strategy for the parameter values used in the model for each state. In Section 4, we present and describe the results of the model for each of the five selected states in the competitive equilibrium scenario. In Section 5, we solve the Ramsey policy problems and analyze the optimal containment rate results for each state. In Section 6, we analyze for each state the implications of adopting optimal containment rates when compared to the baseline scenario of competitive equilibrium. In Section 7 we present the *ex-post* comparison of model results with real-world data. Finally, Section 8 concludes.

2. The SIR-macro model

In this section, we describe with some adaptations the full version of the SIR-macro model as developed by Eichenbaum et al. (2020). The adaptations were necessary because in Eichenbaum et al. (2020) the complete version of the model is constructed with the gradual inclusion of extensions to the basic SIR-macro model along the sections of the article. As in this work we are only interested in the full version of the model, we have adapted the exposition to present it in a single section. The full version of the model includes three main characteristics: the endogenous mortality rate as a function of the infected population, the possibility of discovering effective treatments that cure the infected population, and the possibility of discovering vaccines.

2.1. The economic framework and the pre-infection economy

The population of the economy is represented by a continuum of *ex-ante* identical agents with measure one. These agents maximize the objective function:

$$U = \sum_{t=0}^{\infty} \beta_t u(c_t, n_t). \tag{1}$$

Here $\beta \in (0,1)$ denotes the discount factor and c_t and n_t denote consumption and hours worked, respectively. For simplicity, we assume that momentary utility takes the form

$$u(c_t, n_t) = lnc_t - \frac{\theta}{2} n_t^2. \tag{2}$$

The budget constraint of the representative agent is:

$$(1 + \mu_t)c_t = w_t n_t + \Gamma_t. \tag{3}$$

Here, w_t denotes the real wage rate, μ_t is the tax rate on consumption and Γ_t denotes lump-sum transfers from the government. As discussed in Eichenbaum et al. (2020), μ_t is thought as a proxy for containment measures aimed at reducing social interactions. For this reason, this parameter is referred as the containment rate.[2]

The first-order condition for the representative-agent's problem is:

$$(1 + \mu_t)\theta n_t = c_t^{-1} w_t. \tag{4}$$

There is a continuum of competitive representative firms of unit measure that produce consumption goods (C_t) using hours worked (N_t) according to the technology:

$$C_t = AN_t. \tag{5}$$

The firm chooses hours worked to maximize its time-t profits Π_t:

$$\Pi_t = AN_t - w_t N_t. \tag{6}$$

The government's budget constraint is given by:

$$\mu_t c_t = \Gamma_t. \tag{7}$$

In equilibrium, $n_t = N_t$ and $c_t = C_t$.

2.2. The epidemiological framework and the outbreak of an epidemic

The population is divided into four groups: susceptible, infected, recovered, and deceased. People who have not yet been exposed to the disease are classified as susceptible. People who contracted the disease are classified as infected. People who survived the disease and acquired immunity are classified as recovered. Finally, people who died from the disease are classified as deceased. The fractions of people in these four group, at time-t, are denoted by S_t, I_t, R_te D_t, respectively. The number of newly infected at time-t is denoted by T_t.

[2] Containment rates are proxies for containment measures or containment policies adopted by public authorities. Thus, when we refer to increases or reductions in containment policies or containment measures, we are indirectly referring, in light of the model, to increases or relaxations in the containment rates. All of these terms, for practical purposes, are used interchangeably in this work.

Susceptible people can become infected in three ways: i) meeting infected people while purchasing consumption goods; ii) meeting at work or iii) meeting in ways not directly related to consuming or working, for example in the public transport, meeting a neighbor, at home or touching a contaminated surface.

The number of newly infected people that results from the consumption activities is given by $\pi_1(S_t C_t^s)(I_t C_t^i)$. The terms $S_t C_t^s$ e $I_t C_t^i$ represent total consumption expenditures by susceptible and infected people, respectively. The parameter π_1 reflects both the amount of time spent shopping and the probability of becoming infected as a result of that activity.

The number of newly infected people that results from interactions at work is given by $\pi_2(S_t N_t^s)(I_t N_t^i)$. The terms $S_t N_t^s$ and $I_t N_t^i$ represent total hours worked by susceptible and infected people, respectively. The parameter π_2 reflects the probability of becoming infected as a result of work interactions.

The number of newly infected people that results from the activities not directly related to consuming or working is given by $\pi_3 S_t I_t$. The term $S_t I_t$ represent the number of random meetings between infected and susceptible people. The parameter π_3 reflects the probability of becoming infected as a result of these activities.

The total number of newly infected people is given by:[3]

$$T_t = \pi_1(S_t C_t^s)(I_t C_t^i) + \pi_2(S_t N_t^s)(I_t N_t^i) + \pi_3 S_t I_t. \tag{8}$$

The number of infected people at time $t+1$ is equal to the number of infected people at time t (I_t) plus the number of newly infected (T_t) minus the number of infected people that recovered ($\pi_r I_t$) and the number of infected people that died ($\pi_d I_t$):

$$I_{t+1} = I_t + T_t - (\pi_r + \pi_d) I_t, \tag{9}$$

Here, π_r is the rate at which infected people recover from the infection and π_d is the mortality rate, that is the probability that an infected person dies. To incorporate the effect of the efficacy of the healthcare system in the model, this probability is modeled as a convex function of the fraction κ of the population that becomes infected:

$$\pi_{dt} = \pi_d + \kappa I_t^2. \tag{10}$$

The timing convention in Eq. (9) is as follows. Social interactions happen in the beginning of the period, when infected and susceptible people meet. Then, changes in health status unrelated to social interactions (recovery and death) occur. Finally, at the end of the period the consequences of social interactions materialize: T_t susceptible people become infected.

The number of recovered people at time $t+1$ is the number of recovered people at time t (R_t) plus the number of infected people who just recovered ($\pi_r I_t$):

$$R_{t+1} = R_t + \pi_r I_t. \tag{11}$$

Finally, the number of deceased people at time $t+1$ is the number of deceased people at time t (D_t) plus the number of new deaths ($\pi_{dt} I_t$):

$$D_{t+1} = D_t + \pi_{dt} I_t. \tag{12}$$

The total population evolves according to:

$$POP_{t+1} = POP_t - \pi_{dt} I_t, \tag{13}$$

$$\text{with} \quad POP_0 = 1.$$

The model assumes that at time zero, a fraction ε of susceptible people is infected by a virus through zoonotic exposure, that is the virus is directly transmitted from animals to humans,

$$I_0 = \varepsilon, \tag{14}$$

$$S_0 = 1 - \varepsilon. \tag{15}$$

Everybody is aware of the initial infection and understand the laws of motion governing population heath dynamics. Critically, they take as given aggregate variables like $I_t C_t^i$ and $I_t N_t^i$.

We now describe the optimization problem of different types of people in the economy, as formulated by Eichenbaum et al. (2020). The variable U_t^j denotes the time-t lifetime utility of a type-j agent ($j = s, i, r$). The budget constraint of a type-j person is

$$(1 + \mu_t) c_t^j = w_t \phi^j n_t^j + \Gamma_t, \tag{16}$$

where c_j and n_t^j denote the consumption and hours worked of an agent of type j, respectively. The parameter governing labor productivity, ϕ^j, is equal to one for susceptible and recovered people ($\phi^s = \phi^r = 1$) and less than one for infected people ($\phi^i < 1$).

Susceptible people. The lifetime utility of a susceptible person, U_t^s, is

$$U_t^s = u(c_t^s, n_t^s) + (1 - \delta_v)[(1 - \tau_t)\beta U_{t+1}^s + \tau_t \beta U_{t+1}^i] + \delta_v \beta U_{t+1}^r. \tag{17}$$

[3] Note that the Kermack and McKendrick's (1927) canonical SIR model is a special case of the SIR-macro model in which the propagation of the disease is unrelated to economic activity. This case is characterized by parametric values $\pi_1 = \pi_2 = 0$.

Critically, susceptible people understand that consuming and working less reduces the probability of becoming infected. The variable τ_t represents the probability that a susceptible person becomes infected:

$$\tau_t = \pi_1 c_t^s (I_t C_t^I) + \pi_2 n_t^s (I_t N_t^I) + \pi_3 I_t. \tag{18}$$

The parameter δ_v represents the probability that a vaccine is discovered. With probability $1 - \delta_v$ a person susceptible at time t remains susceptible at time $t + 1$. With probability δ_v this person is vaccinated and becomes immune to the disease. So, at time $t + 1$, this person's health situation is identical to that of a recovered person. The vaccine has no impact on people who were infected or have recovered.

The first-order conditions for consumption and hours worked are:

$$u_1(c_t^s, n_t^s) - (1 + \mu_t)\lambda_{bt}^s + \lambda_{\tau t}\pi_1(I_t C_t^I) = 0, \tag{19}$$

$$u_2(c_t^s, n_t^s) + w_t \lambda_{bt}^s + \lambda_{\tau t}\pi_2(I_t N_t^I) = 0. \tag{20}$$

Here, λ_{bt}^s and $\lambda_{\tau t}$ are the Lagrange multipliers associated with constraints (*16*) and (*18*), respectively.

The first-order condition for τ_t is:

$$\beta(U_{t+1}^i - U_{t+1}^s) - \lambda_{\tau t} = 0. \tag{21}$$

Infected people. The lifetime utility of an infected person, U_t^i, is

$$U_t^i = u(c_t^i, n_t^i) + (1 - \delta_c)[(1 - \pi_r - \pi_d)\beta U_{t+1}^i + \pi_r \beta U_{t+1}^r] + \beta\delta_c U_{t+1}^r. \tag{22}$$

The expression for U_t^i embodies a common assumption in macro and health economics that the cost of death is the foregone utility of life.

The parameter δ_c represents the probability that an effective treatment that cures infected people is discovered each period. Once discovered, treatment is provided to all infected people in the period of discovery and all subsequent periods transforming them into recovered people. As a result, the number of new deaths from the disease goes to zero.

The first-order conditions for consumption and hours worked are given by:

$$u_1(c_t^i, n_t^i) = \lambda_{bt}^i(1 + \mu_t), \tag{23}$$

$$u_2(c_t^i, n_t^i) = -\phi^i w_t \lambda_{bt}^i, \tag{24}$$

where λ_{bt}^i is the Lagrange multiplier associated with constraint (*16*).

Recovered people. The lifetime utility of a recovered person, U_t^r, is

$$U_t^r = u(c_t^r, n_t^r) + \beta U_{t+1}^r. \tag{25}$$

The first-order conditions for consumption and hours worked are:

$$u_1(c_t^r, n_t^r) = \lambda_{bt}^r(1 + \mu_t), \tag{26}$$

$$u_2(c_t^r, n_t^r) = -w_t \lambda_{bt}^r, \tag{27}$$

where λ_{bt}^r is the Lagrange multiplier associated with constraint (*16*).

Government budget constraint. The government budget constraint is

$$\mu_t(S_t c_t^s + I_t c_t^i + R_t c_t^r) = \Gamma_t(S_t + I_t + R_t). \tag{28}$$

Equilibrium. In equilibrium, each person solves their maximization problem and the government budget constraint is satisfied. In addition, the goods and labor markets clear:

$$S_t C_t^s + I_t C_t^i + R_t C_t^r = AN_t, \tag{29}$$

$$S_t N_t^s + I_t N_t^i \phi^i + R_t N_t^r = N_t. \tag{30}$$

3. Calibration

In this section we present our calibration strategy used to determine the model parameters for each of the five chosen states, namely, São Paulo (SP), Amazonas (AM), Ceará (CE), Rio de Janeiro (RJ) and Pernambuco (PE). As already mentioned, the model was originally calibrated in May 2020. The results were then published as a working paper in its English version in June 2020 (Borelli and Góes, 2020a) and in its Portuguese version in August 2020 (Borelli and Góes, 2020b). The final values of the calibrated parameters are presented in Tables 1 and 2.

First of all, we need to state an important consideration regarding the time convention adopted for the model results. As the main purpose of the model was not to compute point-in-time quantitative predictions about issues such as the peak date of the infected population, we decided to give up defining a specific time periodicity for the model. Instead, we chose to normalize the

Table 1
Main values used for the calibration of the parameters and variables of each state.

Value	SP	AM	CE	RJ	PE
Imperial College's Estimated IFR (%)	0.70	0.80	1.10	0.80	1.10
Number of Workers	22,782,714	1,657,700	3,764,280	7,651,617	3,602,820
Number of Students	10,306,000	1,284,000	2,376,000	3,853,000	2,475,000
Average time devoted to household chores (daily hours)	2.06	1.44	1.87	2.04	2.02
Average number of people per residence	2.80	3.60	3.10	2.70	2.90
Average time spent in public transport (minutes)	37.15	33.95	26.60	43.07	30.52
Pre-epidemic population	45,919,049	4,144,597	9,132,078	17,264,943	9,557,071
Average time devoted to work (daily hours)	8.24	7.30	7.58	8.10	7.74
Per capita income	1,889	838	939	1,809	954

Table 2
Calibrated values for the main variables and parameters of each state.

Parameter/Variable	SP	AM	CE	RJ	PE
κ	0.63	1.10	2.35	1.33	1.90
α_1	0.16	0.28	0.30	0.12	0.25
α_2	0.17	0.13	0.14	0.16	0.14
α_3	0.66	0.60	0.56	0.71	0.61
π_1	$4.28{\cdot}10^{-7}$	$3.68{\cdot}10^{-6}$	$3.17{\cdot}10^{-6}$	$8.53{\cdot}10^{-7}$	$2.59{\cdot}10^{-6}$
π_2	$5.99{\cdot}10^{-5}$	$5.54{\cdot}10^{-5}$	$5.85{\cdot}10^{-5}$	$5.13{\cdot}10^{-5}$	$5.33{\cdot}10^{-5}$
π_3	0.39	0.35	0.33	0.33	0.36
ε	$\frac{100}{45,919,049}$	$\frac{100}{4,144,597}$	$\frac{100}{9,132,078}$	$\frac{100}{17,264,943}$	$\frac{100}{9,557,071}$
A	11.46	5.74	6.19	11.17	6.16
θ	$5.89{\cdot}10^{-4}$	$7.51{\cdot}10^{-4}$	$6.96{\cdot}10^{-4}$	$6.10{\cdot}10^{-4}$	$6.68{\cdot}10^{-4}$
β	0.966	0.966	0.966	0.966	0.966
ϕ^i	0.80	0.80	0.80	0.80	0.80

total duration of the time interval for which the exercises were computed to unit. Thus, the time interpretation of the model became in relation to the progress (%) of the total duration of the epidemics. Therefore, as the total duration of the epidemics will only be known *ex-post*, we exempted the work from any predictive responsibilities that could be attributed to it and emphasize the qualitative and comparative nature of its results.

To calibrate the value of κ for each state we used infection fatality rate estimates from Mellan's et al. (2020) Report 21 from Imperial College for a series of Brazilian states. We calibrated the values of κ for each of the five states so that the mortality rates in the competitive equilibrium peaks at the values of these estimated infection fatality rates. Although the mortality rates are endogenous to the model, they need an initial value. Following Rabelo and Soares (2020) we used 0.3% as the initial mortality rate for all states. This value was obtained as a weighted average of the mortality rates verified in South Korea (the country that had the world's highest per capita test rates for COVID-19) using weights equal to the percentage of the Brazilian population for different age groups.[4]

Proceeding with our calibration strategy for π_1, π_2, and π_3 for each state, we started by adopting the same premise of Eichenbaum et al. (2020) that, as is common in epidemiology, the relative importance of different modes of transmission is similar across viruses that cause respiratory diseases. Ferguson et al. (2006) argued that, in the case of influenza, 30% of transmissions occur in the household, 33% in the general community, and 37% occur in schools and workplaces. Based on this assumption adopted, we used these percentages as the basis for our calibration.

As in Eichenbaum et al. (2020), we calibrated the values of π_1, π_2, and π_3 to satisfy the system

$$\begin{aligned}
\frac{\pi_1 C^2}{\pi_1 C^2 + \pi_2 N^2 + \pi_3} &= \alpha_1 \\
\frac{\pi_2 N^2}{\pi_1 C^2 + \pi_2 N^2 + \pi_3} &= \alpha_2 \\
\frac{\pi_3}{\pi_1 C^2 + \pi_2 N^2 + \pi_3} &= \alpha_3
\end{aligned} \tag{31}$$

[4] The decision to use the South Korean mortality rate was made due to the scarcity of data at the time of the original calibration (May 2020, as discussed above). Now, however, there is already data available for Brazil regarding this parameter, so that it could be recalibrated. To offset our decision not to recalibrate the model (see Section 7 for a more in-depth discussion of this decision), we have provided a sensitivity analysis in Appendix A.4 of initial mortality rates for all five states that make possible an assessment of how alternative calibrations for the initial mortality rate could potentially affect the model results.

where C and N are the consumption and hours worked in the pre-epidemic steady state. Note that α_1, α_2, and α_3 are the shares of transmissions that occur in consumption, at work and in other activities, respectively. Having these shares calibrated, it is possible to solve the system and therefore obtain the values of π_1, π_2, and π_3. Thus, it is easy to see that the calibration problem of π_1, π_2, and π_3 is equivalent to the calibration problem of α_1, α_2, and α_3. Also note that as $\alpha_1 + \alpha_2 + \alpha_3 = 1$, it is enough that two of the portions are calibrated for the latter to be obtained residually.

Due to the lack of data available for Brazil, it became impractical to calibrate α_1 directly. We then choose to calibrate α_2 and α_3 and obtain α_1 residually. We calibrated the share of transmissions that occur at work, α_2, using the same approach as Eichenbaum et al. (2020). We weighted the number of students and workers in each state by 10 and 4, respectively. These weights refer to the average amount of physical contacts per day at school and at work, obtained from Lee et al. (2010). For the total number of workers, we used the number of persons aged 14 and over employed in the labor force obtained from IBGE.[5] For the total number of students, we used the number of students aged 4 and over, also obtained from IBGE.[6]

It is worth noting that in Brazil what ended up happening was that almost all schools were closed during the pandemic. Given this fact, a valid question would be: if we included this pattern of school closures in the model, would the model's results change? Imposing a pattern of closing schools would mean affecting the value of α_2, reducing it. Keeping the calibration of α_3 fixed, this would imply an increase of α_1, since $\alpha_1 + \alpha_2 + \alpha_3 = 1$.We provide in Appendix A.1, for all states, a sensitivity analysis following this logic, so that it is possible to evaluate how alternative calibrations of α_2 could affect the model results.[7]

Proceeding, we calibrated the share of infections that occur in other activities, α_3, using some calibration hypothesis and data on i) the proportion of daily hours dedicated to household chores of persons aged 14 and over; ii) the average number of people per household and iii) the usual time of commuting of individuals to work.[8] Having the values of α_2 and α_3 calibrated, we obtained the value of α_1 residually and, with these three calibrated fractions, we finally obtained π_1, π_2, and π_3 by solving system (31). More technical details regarding the calibration of α_1, α_2, and α_3 can be found in Borelli and Góes (2020a, 2020b) technical appendix.

The initial population was normalized to one. For each state, we calibrated the number of people that are initially infected to represent a number of 100 infected people at $t = 0$. Thus, for each state ε was calculated as:

$$\varepsilon = \frac{100}{POP} \tag{32}$$

where POP is the estimated resident population for 2019 for the state, obtained from IBGE.[9] Calibrating in this way for each state, it was possible to capture and compare the effect of the different population sizes of each state on the local dynamics of the epidemic.

As in Eichenbaum et al. (2020), we calibrated the values of A and θ so that in the pre-epidemic steady state the representative person of each state works the average hours worked by the population of his state and earns the per capita income of the population of his state. For this, we used the average hours usually worked per week in all jobs of people aged 14 and over and the average real monthly household income per capita, at average prices of the year, for each of the states. The first data set was obtained from IBGE[10] and the latter from 2019 *PNAD Contínua* survey.

To calibrate the discount factor, β, for all states we used the same value calculated by Rabelo and Soares (2020) for Brazil. This value is equivalent to a statistical value of life of R$ 2,9 million. As indicated by these authors, this value is based on recent estimates for Brazil by Ferrari et al. (2019) and Rocha et al. (2019).

Again, as in Eichenbaum et al. (2020), we calibrated the parameter that controls the relative productivity of infected people, ϕ^i, as 0.8. This value is consistent with the notion that symptomatic agents don't work and the assumption that 80% of infected people are asymptomatic according to the China Center for Disease Control and Prevention.

Regarding the probabilities of discovering effective treatments and vaccines, δ_c and δ_v, respectively, following Eichenbaum et al. (2020) we calibrated them to reflect an average discovery time of one year.

4. Competitive equilibrium

In this first exercise, we present results for the competitive equilibrium of each state. In the competitive equilibrium, there are no attempts by the authorities to contain the evolution of the epidemic. The dynamics of the epidemic are affected only by the decisions made by economic agents, that are free to reduce their chances of being infected by reducing consumption and hours worked.

In this and the next sections, we illustrate the differences between states by describing the main results for each variable. To keep text clarity, we describe the results only for the states that presented the highest and lowest values for each variable. These values will be sufficient to assess the size of the heterogeneity of results between states. Nevertheless, the other results can be

[5] *Sistema IBGE de Recuperação Automática* (IBGE Automatic Recovery System), Table 4093.
[6] *Sistema IBGE de Recuperação Automática* (IBGE Automatic Recovery System), Table 983.
[7] In general terms, the sensitivity analysis shows that, for all states, the qualitative consequences of a reduction of α_2 (through the closing of schools, for example) would be a reduction in the mortality rate, in the peak of infected people and in the total deaths by the end of the epidemic, as well as a reduction in the size of the economic recession. Increases of α_2, on the other hand, would have the similarly opposite effect.
[8] Due to the importance of this parameter (α_3) and its calibration complexity, we also present in Appendix A.2 a sensitivity analysis for its possible values.
[9] *Sistema IBGE de Recuperação Automática* (IBGE Automatic Recovery System), Table 6579.
[10] *Sistema IBGE de Recuperação Automática* (IBGE Automatic Recovery System), Table 6373.

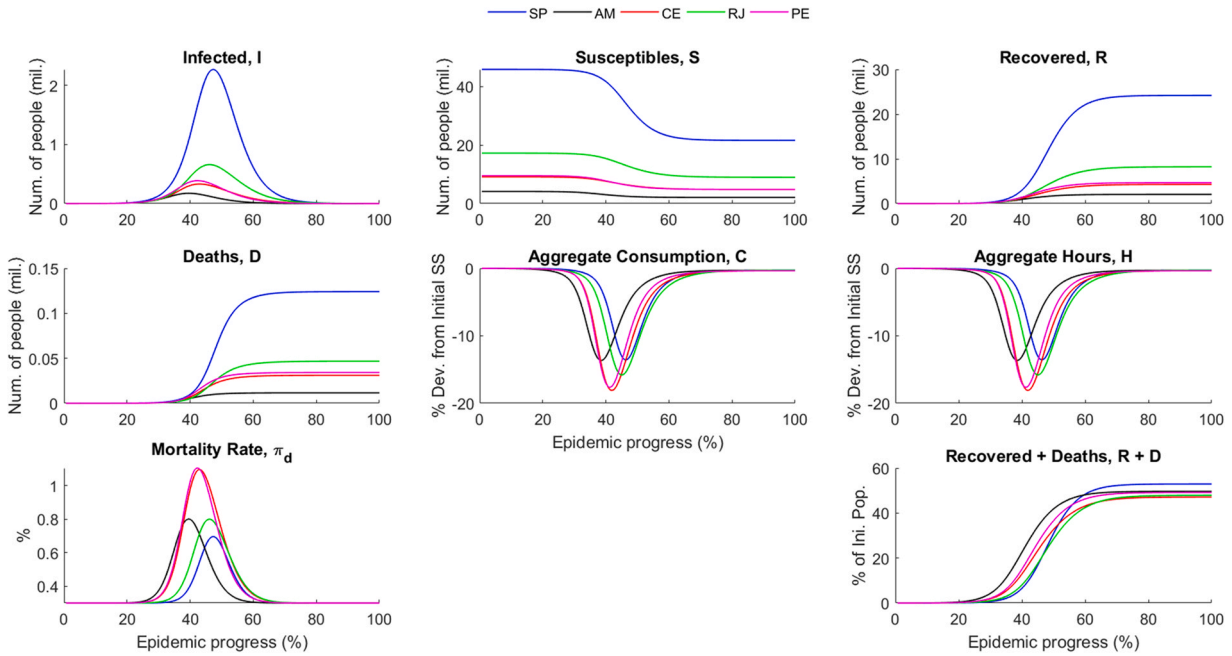

Fig. 1. SIR-macro model - Results for competitive equilibrium, in level.

analyzed in greater detail in the figures and tables that will be presented by the end of the article. All numerical results will be summarized in Table 3, in Section 5. Regarding this section, Fig. 1 shows, in level, the dynamics of the evolution of the epidemic for each of the five states, as well as its effects on the aggregates of consumption and hours worked in each of them, for the competitive equilibrium. Fig. 2 shows the same results but in proportion (%) to the initial population of each state.

Proceeding to the results, first, we can observe that the state that reaches the highest peak of the infected share of the pre-epidemic population is the state of São Paulo (SP), at 4.95%. At the other extreme, the state that reaches the lowest peak is the state of Ceará (CE), with 3.83% of the pre-epidemic population infected. In relation to the temporal dimension, the peak of

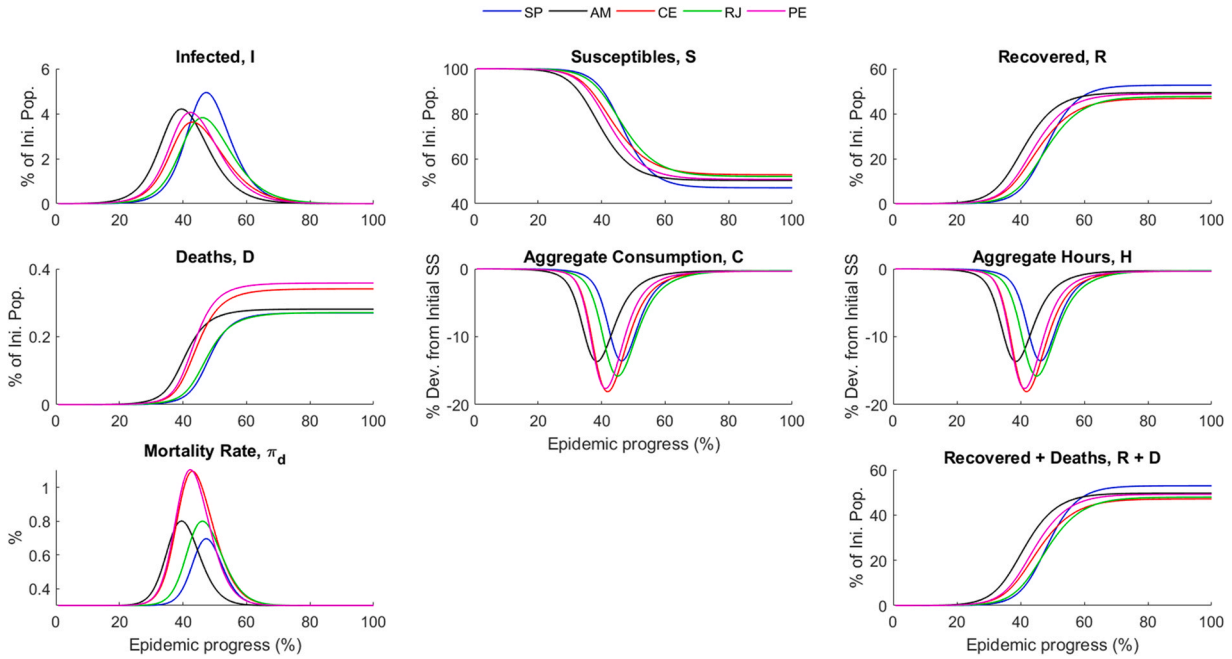

Fig. 2. SIR-macro model – Results for competitive equilibrium, in percentage of the initial population.

infected people occurs first in Amazonas (AM), with 39.33% of the progress of the total time of the epidemic occurred and, only lastly, in São Paulo (SP), with 47.33% of the time progress of the epidemic occurred.

Concerning the macroeconomic consequences of the epidemic, among the five states analyzed, the most severe macroeconomic shock occurs in Ceará (CE), where the aggregates of consumption and hours worked offered suffer a fall of approximately 18.11% in comparison to the pre-epidemic steady state. On the other hand, the least severe occurs in São Paulo (SP), where the falls in aggregate consumption and the aggregate hours of work reached a trough of −13.55%. Regarding time, the recession trough occurs first in Amazonas (AM), when the progress of the total duration of the epidemic reaches 38.67% and, lastly, in São Paulo (SP), when the progress of the total duration of the epidemic reaches 46.00%, 8.67 percentage points of the progress of the epidemic after Amazonas (AM).

The epidemic ends with 52.93% of the population of São Paulo (SP) infected, the largest share of the population infected among the five states analyzed in the competitive equilibrium. On the other hand, Ceará (CE) has the lowest share among the five states, with 47.12% of the population infected at the end of the epidemic. As a consequence of the infections, the state with the largest share of the initial population affected by death is the state of Pernambuco (PE), with 0.36%, while those with the smallest shares are the states of Rio de Janeiro (RJ) and São Paulo (SP), both with 0.27%.

These sample results illustrate evidence of relevant differences in the epidemic dynamics of each state in the competitive equilibrium due to its intrinsic differences. It is possible to note that the size of the infected peak and the time required to reach it are significantly different in each state. The depth and duration of recessions, the share of the total population infected and the share of the population affected by death at the end of the epidemic in each state also differ between them.

In the next section, we analyze optimal containment policies that can be adopted by states to improve the results obtained in competitive equilibrium. Our main interest is to analyze how these containment policies differ between these states. In Section 6 we analyze the results under the scenario of adopting these policies and compare them against the results presented in this section to assess the effects of adopting these measures.

5. Optimal containment policy

In this section, inspired by Eichenbaum et al. (2020), we consider a simple Ramsey problem to deal with a classic externality associated with the behavior of infected agents in the competitive equilibrium. Because agents are atomistic, they don't take into account the impact of their actions on the infection and death rates of other agents. For this reason, the competitive equilibrium is not socially optimal.

Eichenbaum et al. (2020), analogous to Farhi and Werning, 2020 treatment of capital controls, model the containment measures as a tax on consumption, the proceeds of which are rebated lump sum to all agents. This tax on consumption is referred as the containment rate. We proceed, as well as Eichenbaum et al. (2020), modeling in this way.

In this section we compute, for each state, the optimal sequence of 250 containment rates $\{\mu_t\}_{t=0}^{249}$ that maximize social welfare, U_0, defined as a weighted average of the lifetime utility of the different agents. Since at time zero $t = 0$, $R_0 = D_0 = 0$, the value of U_0 is

$$U_0 = S_0 U_0^s + I_0 U_0^i. \tag{33}$$

Given the sequence of containment rates, we solve for the competitive equilibrium and evaluate the social welfare function. We iterate on this sequence until we find the optimum.

Fig. 3 shows the results, in level, for which all states adopt optimal containment policies. Fig. 4 shows the same results, but as percentage of the initial population.

First, we can see that in the period $t = 0$, where the infected population in each state reaches the level of 100 individuals, the containment rates are already high for all five states. The highest initial containment rate occurs in Ceará (CE), at 16.12%, while the lowest in São Paulo (SP), at 14.05%.

As the containment rates evolve, the state that reaches the highest peak of the containment rate among the five states is the state of Pernambuco (PE), with a containment rate of 53.40%. On the other hand, São Paulo (SP) is the state with the lowest peak containment rate, at 38.76%. These numbers illustrate the alarming size of heterogeneity between states in terms of the level to which containment should be taken. The state of Pernambuco (PE) requires that the containment rate be raised 14.64 percentage points more than in São Paulo (SP).

Regarding time, the peak of the containment rate occurs first in the state of Amazonas (AM), in 40.67% of the progress of the total time of the epidemic, this being, therefore, the first state to begin to relax the containment measures. On the other hand, the peak occurs lastly in Rio de Janeiro (RJ), with 48.67% of the progress of the epidemic occurred. Rio de Janeiro (RJ) is, therefore, the last state to start the process of gradual relaxation of containment measures. These results illustrate how the optimal duration and speed of containment policies can vary across states.

In summary, these results illustrate that the intrinsic differences of each state not only affect the initial severity of the containment measures adopted by each of them but also the dynamics of the evolution of these containment rates over time, implying differences in i) the ideal moment when the measures containment will need to be raised, ii) how far they will need to be raised and iii) when they can finally be relaxed. Notwithstanding these interstate differences in the optimal conduct of containment policies, all results indicate that the adoption of relatively severe containment measures was an optimal decision for each of the five states.

In this section, we studied the optimal containment policies to be adopted by each of the five states analyzed. However, the implications of adopting these optimal policies have not been analyzed. In the next section, these implications (in comparison to the competitive equilibrium set out in the previous section) are analyzed under various dimensions.

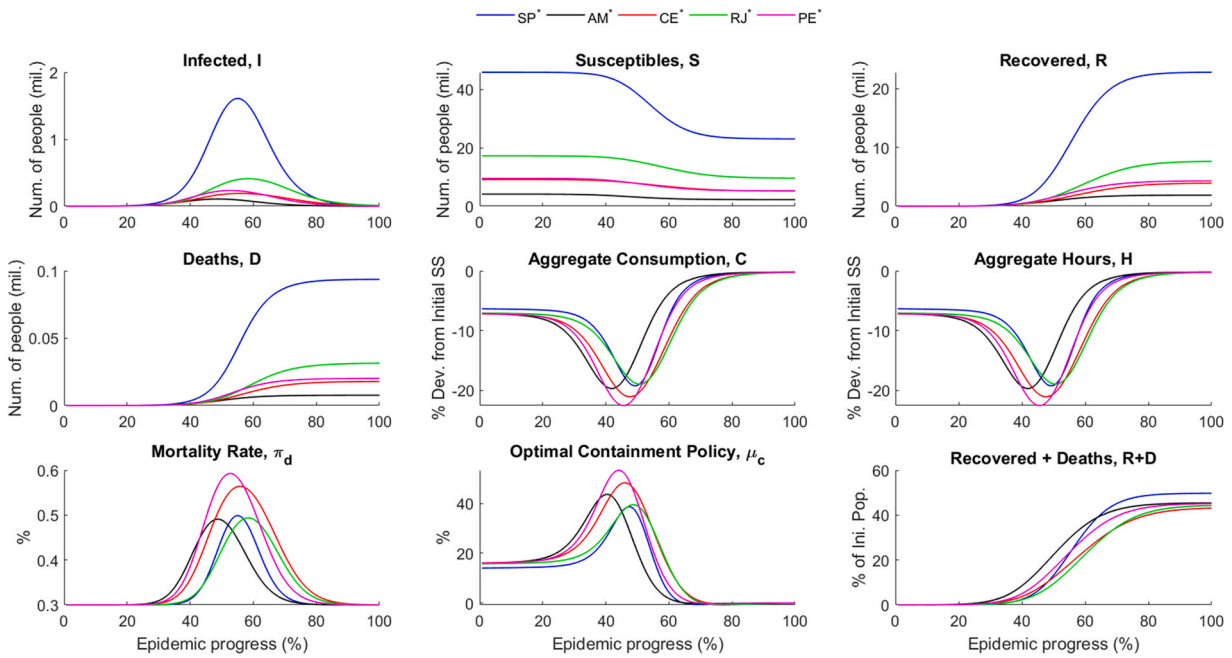

Fig. 3. SIR-macro model - Results under the adoption of optimal containment policies, in level.

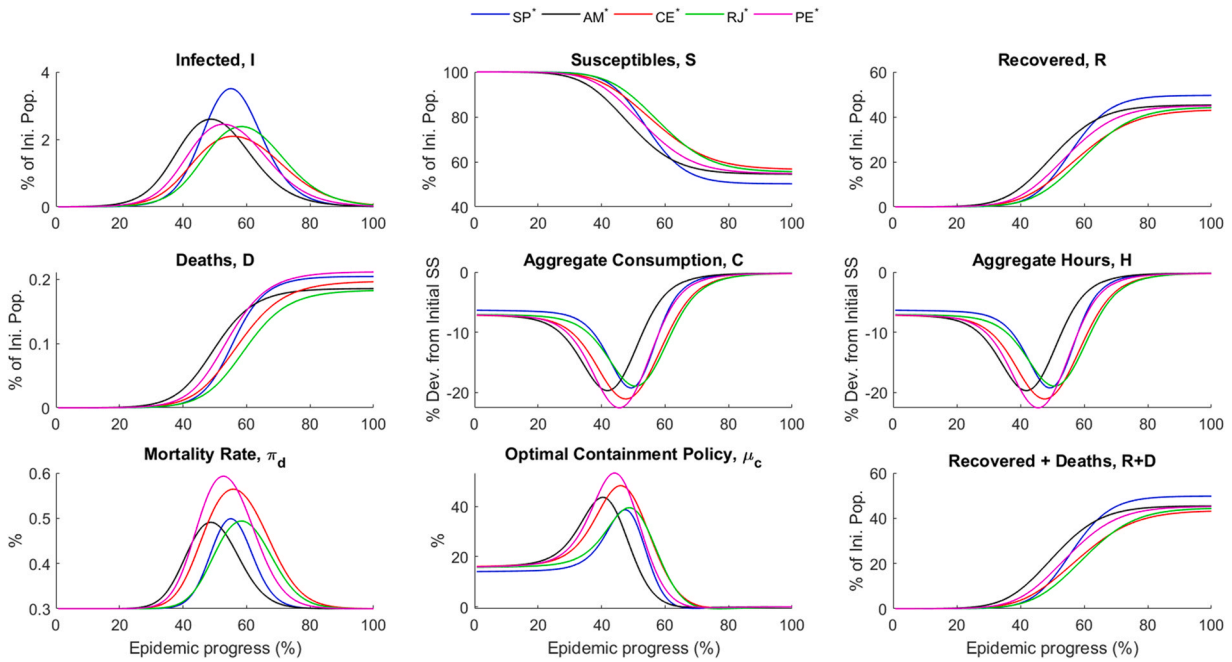

Fig. 4. SIR-macro model – Results under the adoption of optimal containment policies, in percentage of the initial population.

6. The implications of optimal containment policies

All the results that will be described in this section are summarized in Table 3. Table 4 summarizes the effects of the adoption of optimal containment policies by the states in comparison to the competitive equilibrium scenario. Table 5 shows, for each scenario, the moments of the progress of the epidemic when the main peaks and troughs in the results of each state occur.

In the scenario under the adoption of optimal containment policies, the state with the largest share of the population infected at the peak is São Paulo (SP), at 3.50%. On the other hand, the lowest is the state of Ceará (CE), at 2.09%. In comparison to the

Table 3
Results for the main variables of the model for the competitive equilibrium and optimal policy scenarios.

Variable	Scenario	São Paulo (SP)		Amazonas (AM)		Ceará (CE)		Rio de Janeiro (RJ)		Pernambuco (PE)	
Total uninfected by the end of the epidemic, S	**Competitive Eq.**	21,614,655.03	(47.07%)	2,086,398.55	(50.34%)	4,828,940.12	(52.88%)	8,999,825.11	(52.13%)	4,858,460.45	(50.84%)
(Number of people. In parentheses: percentage of initial population)	**Optimal Policy**	23,073,448.23	(50.25%)	2,261,651.74	(54.57%)	5,189,707.29	(56.83%)	9,607,865.98	(55.65%)	5,242,447.63	(54.85%)
Peak infected population, I	**Competitive Eq.**	2,271,910.63	(4.95%)	174,441.47	(4.21%)	331,309.55	(3.63%)	660,399.78	(3.83%)	387,726.67	(4.06%)
(Number of people. In parentheses: percentage of initial population)	**Optimal Policy**	1,608,921.78	(3.50%)	107,708.85	(2.60%)	190,939.73	(2.09%)	410,857.91	(2.38%)	234,004.12	(2.45%)
Total recovered by the end of the epidemic, R	**Competitive Eq,**	24,180,003.96	(52.66%)	2,046,520.78	(49.38%)	4,271,783.72	(46.78%)	8,217,878.32	(47.60%)	4,664,293.18	(48.80%)
(Number of people. In parentheses: percentage of initial population)	**Optimal Policy**	22,747,425.46	(49.54%)	1,874,748.12	(45.23%)	3,918,618.10	(42.91%)	7,615,853.03	(44.11%)	4,291,798.23	(44.91%)
Total deaths by the end of the epidemic, D	**Competitive Eq.**	124,101.88	(0.27%)	11,660.84	(0.28%)	31,144.56	(0.34%)	46,800.59	(0.27%)	34,221.33	(0.36%)
(Number of people. In parentheses: percentage of initial population)	**Optimal Policy**	93,693.42	(0.20%)	7676.48	(0.19%)	17,884.19	(0.20%)	31,433.62	(0.18%)	20,163.66	(0.21%)
Total infected by the end of the epidemic, R+D	**Competitive Eq.**	24,304,105.84	(52.93%)	2,058,181.61	(49.66%)	4,302,928.28	(47.12%)	8,264,678.91	(47.87%)	4,698,514.51	(49.16%)
(Number of people. In parentheses: percentage of initial population)	**Optimal Policy**	22,841,118.88	(49.74%)	1,882,424.60	(45.42%)	3,936,502.30	(43.11%)	7,647,286.65	(44.29%)	4,311,961.89	(45.12%)
Peak mortality rate	**Competitive Eq.**	0.70%		0.80%		1.10%		0.80%		1.10%	
(%)	**Optimal Policy**	0.50%		0.49%		0.56%		0.49%		0.59%	
Aggregate consumption in the trough	**Competitive Eq.**	-13.55%		-13.67%		-18.11%		-15.80%		-17.66%	
(% Dev. from Initial Steady State)	**Optimal Policy**	-19.28%		-19.72%		-21.10%		-18.98%		-22.58%	
Aggregate of hours worked in the trough	**Competitive Eq.**	-13.55%		-13.67%		-18.11%		-15.80%		-17.66%	
(% Dev. from Initial Steady State)	**Optimal Policy**	-19.28%		-19.72%		-21.10%		-18.98%		-22.58%	

Table 4
Effects of the adoption of optimal containment policies by the states in relation to the competitive equilibrium scenario.

Value	SP		AM		CE		RJ		PE	
Peak containment rate (%)	38.76%		43.68%		48.35%		39.54%		53.40%	
Infected people avoided at peak (Number of people. In parentheses: percentage of initial population)	662,989	(1.44%)	66,733	(1.61%)	140,370	(1.54%)	249,542	(1.45%)	153,723	(1.61%)
Total infections avoided (Number of people. In parentheses: percentage of initial population)	1,462,987	(3.19%)	175,757	(4.24%)	366,426	(4.01%)	617,392	(3.58%)	386,553	(4.04%)
Peak mortality rate reduction (%)	-0.20%		-0.31%		-0.53%		-0.31%		-0.51%	
Saved lives (Number of people. In parentheses: percentage of initial population)	30,408	(0.07%)	3984	(0.10%)	13,260	(0.15%)	15,367	(0.09%)	14,058	(0.15%)
Effect on aggregate consumption in the trough (% Dev. From Initial Steady State)	-5.73%		-6.06%		-2.99%		-3.18%		-4.92%	
Effect on aggregate hours worked in the trough (% Dev. From Initial Steady State)	-5.73%		-6.06%		-2.99%		-3.18%		-4.92%	

Table 5
Moments of progress of the epidemic in which the peaks and troughs of the main variables of the model occur in each scenario, for each state.

Value	Scenario	SP	AM	CE	RJ	PE
Moment of progress of the epidemic in which the peak of infected people occurs, I (% progress of the total time of the epidemic)	**Competitive Eq.**	47.33%	39.33%	42.67%	46.00%	42.00%
	Optimal Policy	55.33%	48.67%	56.00%	58.67%	52.67%
Moment of progress of the epidemic when peak containment rate occurs, μ_t (% progress of the total time of the epidemic)	**Optimal Policy**	47.33%	40.67%	46.00%	48.67%	44.00%
Moment of progress of the epidemic when the peak mortality rate occurs, π_d (% progress of the total time of the epidemic)	**Competitive Eq.**	47.33%	39.33%	42.67%	46.00%	42.00%
	Optimal Policy	55.33%	48.67%	56.00%	58.67%	52.67%
Moment of progress of the epidemic when the trough of recession occurs (% progress of the total time of the epidemic)	**Competitive Eq.**	46.00%	38.67%	42.00%	45.33%	41.33%
	Optimal Policy	49.33%	42.00%	47.33%	50.67%	45.33%

competitive equilibrium, with the adoption of optimal policies, the greatest reduction in the infected peak occurs for the states of Amazonas (AM) and Pernambuco (PE), both with the peak of infected individuals reduced by 1.61 percentage points of the pre-epidemic population. At the other extreme, the smallest reduction occurs in São Paulo (SP), of only 1.44 percentage points.

With regard to time, the peak of infected people occurs first in Amazonas (AM), with 48.67% of the progress of the total time of the epidemic occurred, and lastly in Rio de Janeiro (RJ), with 58.67%. In comparison to the competitive equilibrium, the state that suffers the longest extension of time until the peak of infected due to the adoption of optimal containment policies, is the state of Ceará (CE), which has its peak of infected delayed by 13.33 percentage points of the epidemic's progress. At the other extreme, the one that suffers the least prolongation is the state of São Paulo (SP), with a delay of only 8 percentage points in the progress of the epidemic.

Proceeding for macroeconomic shocks, with the adoption of optimal containment policies there is a worsening recession for all states. The biggest recession happens in the state of Pernambuco (PE), with a drop in aggregate consumption and the aggregate of hours worked of 22.58%. The smallest recession occurs in São Paulo (SP), with a fall of 19.28% of the aggregate consumption and aggregate hours worked. In comparison to the results of competitive equilibrium, the state that suffers the least impact on the recession is Ceará (CE), as a deepening of only 3 percentage points of the aggregates' troughs. On the other hand, the one that suffers the greatest deepening is the state of Amazonas (AM), of 6.06 percentage points of the pre-epidemic steady state, more than double the deepening suffered by Ceará (CE).

Observing the temporal dynamics, we can notice that the first state to reach the trough is Amazonas (AM), in 42.00% of the progress of the total time of the epidemic, while the one that finally reaches it is Rio de Janeiro (RJ), in 50.67% of the progress of the total time of the epidemic. In comparison to the competitive equilibrium, the states that suffer the greatest increases in the duration of the recession are the states of Ceará (CE) and Rio de Janeiro (RJ), both with an extension of 5.33 percentage points of the time progress of the epidemic in that the trough of recession occurs. On the other hand, the states that experienced the smallest increases in duration were the states of Amazonas (AM) and São Paulo (SP), both with an extension of only 3.33 percentage points.

At the end of the epidemic, the state with the largest share of the population infected becomes the state of São Paulo (SP), with 49.74%. The state with the smallest becomes the state of Ceará (CE), with 43.11%. In comparison to the competitive equilibrium, the state that suffers the greatest reduction in this share due to the adoption of optimal containment policies is the state of Amazonas (AM), with a reduction of 4.24 percentage points of the share of the total population that is infected. The state that suffers the smallest reduction is the state of São Paulo (SP), with a reduction of 3.19 percentage points of the share of the total population that is infected.

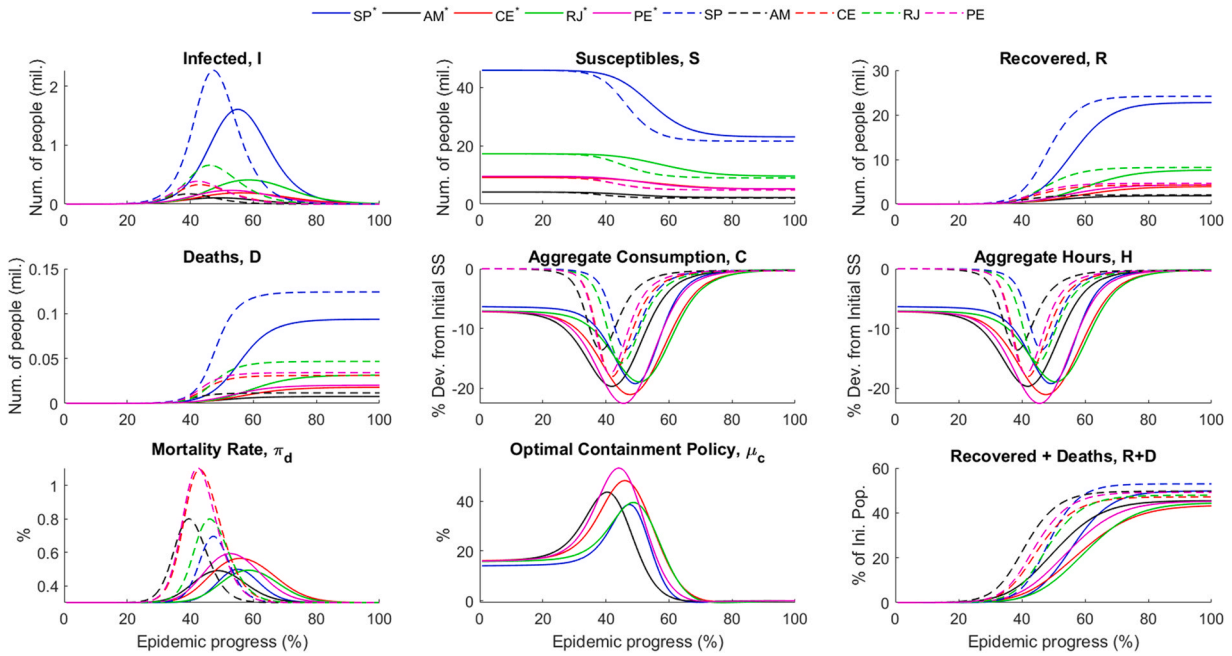

Fig. 5. SIR-macro model – Comparison of results between the scenarios of optimal containment policy (solid line) and competitive equilibrium (dotted lines), in level.

As a result of infections, the largest share of the initial population that dies occurs in Pernambuco (PE), where it reaches 0.21%. The lowest occurs in the state of Rio de Janeiro (RJ), where it reaches 0.18% of the population. In comparison to the competitive equilibrium, the largest reduction in the portion of the population that dies occurs in the state of Pernambuco (PE), of approximately 0.16 percentage points of the pre-epidemic population, while the smallest reduction occurs in São Paulo (SP), of only 0.07 percentage points of the pre-epidemic population, a reduction of less than half that observed in Pernambuco (PE).

These results show evidence that the intrinsic differences between the states significantly influence the effect of adopting optimal containment policies, heterogeneously affecting the peak of the infected curve and its time dynamics, the severity of economic recessions, the share of the total population that is infected at the end of the epidemic and the percentage of the pre-epidemic population that dies.

Fig. 5 shows the comparison of results between the competitive equilibrium and the optimal policy scenario for all states together, in level. Fig. 6 shows the same results but as a percentage of the initial population. Figs. 7-11 show the comparisons of results between the competitive equilibrium and the optimal policy scenario for each of the states separately, in level.

7. One year later: model performance in retrospect

As already mentioned in Section 3, the model presented here was originally calibrated in May 2020, using the scarce data then available at the time. The results were then published as a working paper in its English version in Borelli and Góes (2020a) and its Portuguese version in Borelli and Góes (2020b). At that time, the numbers of cumulative deaths in the states of São Paulo (SP), Amazonas (AM), Ceará (CE), Rio de Janeiro (RJ) and Pernambuco (PE) were, respectively, of approximately 4,700, 1,400, 1,600, 2,600 and 1,500 confirmed deaths. In Brazil as a whole, there were approximately 15,600 confirmed deaths.[11]

Of course, we could recalibrate the model *ex-post* in order to chase the best possible match with the observed data. However, given the context of the pandemic, we decided to take a different approach than usual. We decided not to recalibrate the model and instead present and evaluate the results of the original *ex-ante* calibration, in order to verify the potential contribution that the model had at the most critical and uncertain moments of the pandemic.[12]

[11] More precisely, these numbers refer to the cumulative deaths on 16, May 2020, the exact day when the calibration was finished.

[12] Surely we could now, that most of the pandemic has passed, do a reverse engineering calibration in order to get the best possible match with the data. However, this would say nothing about the value of the model at times when it would be most useful (namely, at times of uncertainty and data scarcity such as at the start of the pandemic). The comparison with the original model (not recalibrated), despite being worse in terms of the match with the data, shows that in the most important moments of the pandemic the model was able to offer reasonable predictions. This, in turn, shows that if the model were constantly recalibrated throughout the pandemic with new data available, it could be a very useful analytical tool. Comparing non-recalibrated results was also the approach adopted by Eichenbaum et al. (2021) in the final published version of their article. They compared the results of the original model (considering the first calibration) with data observed approximately one year later.

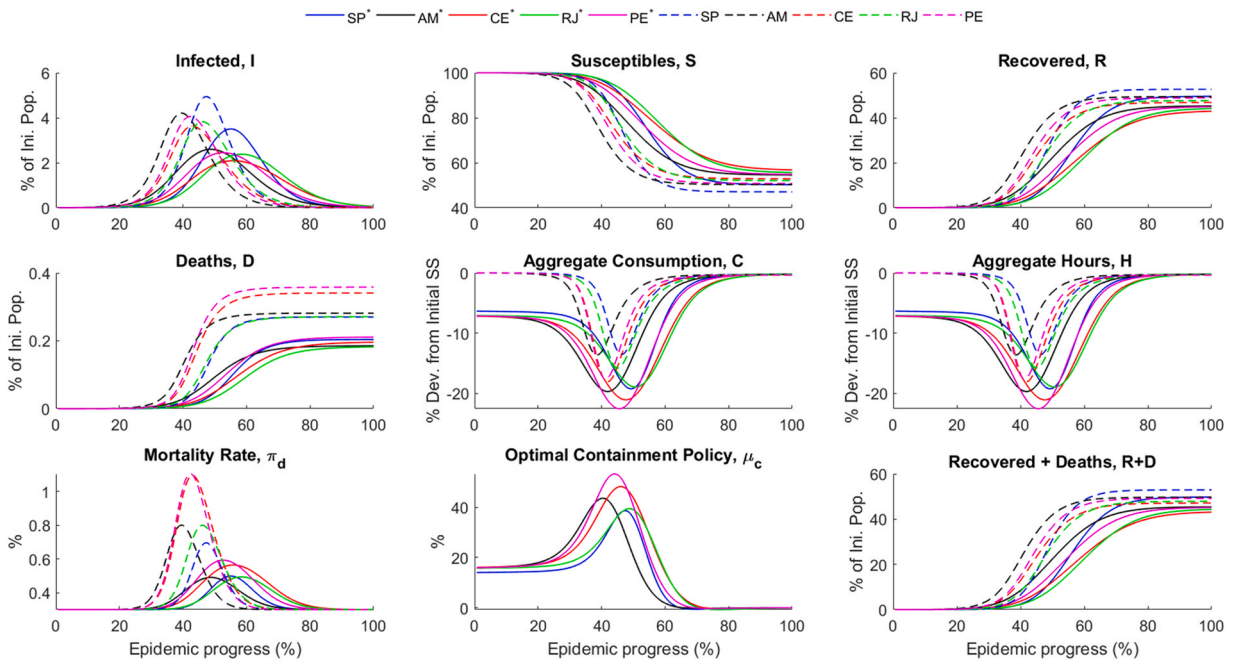

Fig. 6. SIR-macro model – Comparison of results between the scenarios of optimal containment policy (solid line) and competitive equilibrium (dotted lines), in percentage of the initial population.

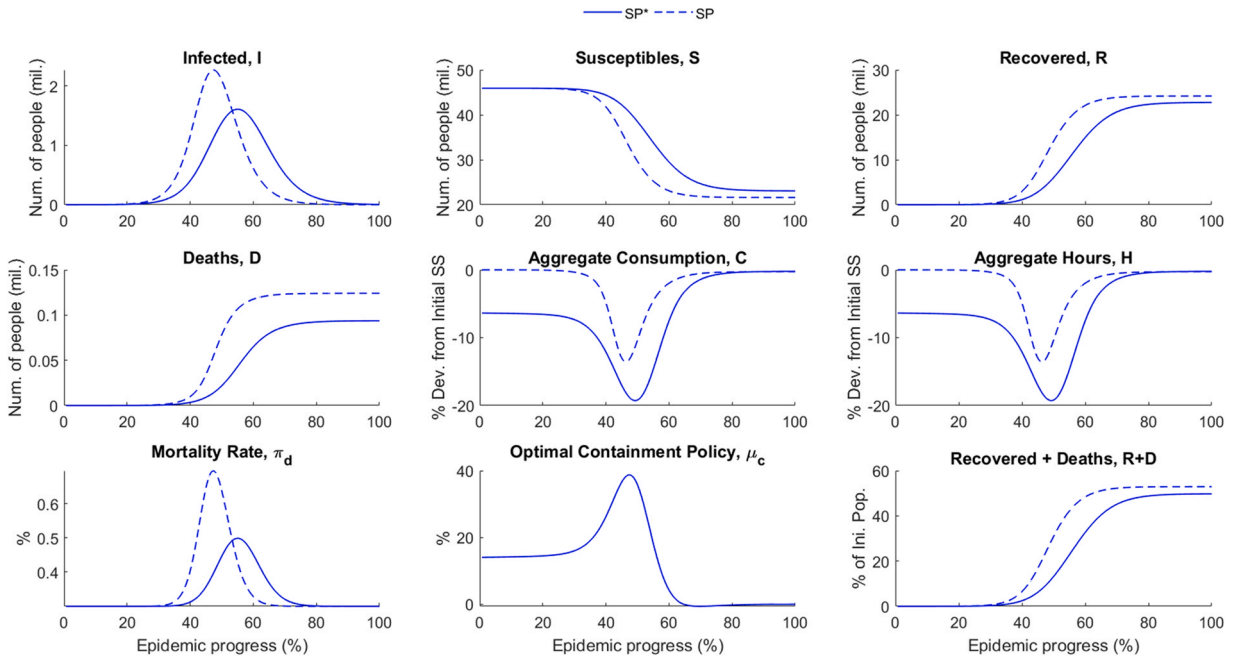

Fig. 7. SIR-macro model – Comparison of results between the scenarios of optimal containment policy (solid line) and competitive equilibrium (dotted lines): São Paulo (SP), in level.

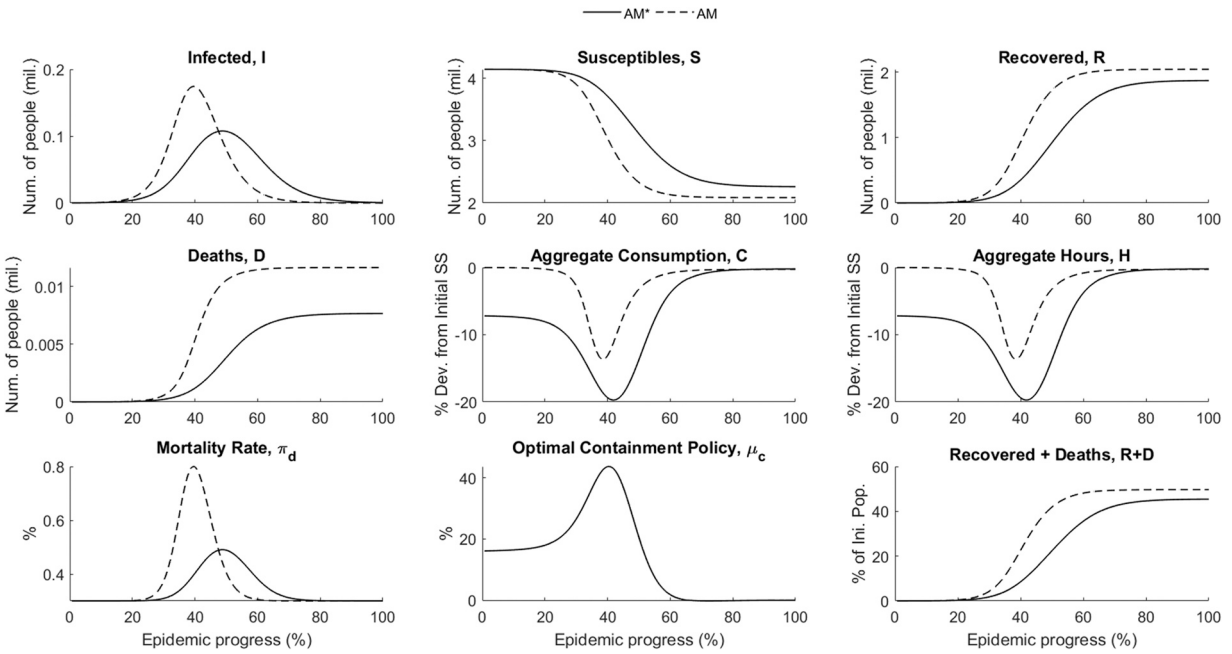

Fig. 8. SIR-macro model – Comparison of results between the scenarios of optimal containment policy (solid line) and competitive equilibrium (dotted lines): Amazonas (AM), in level.

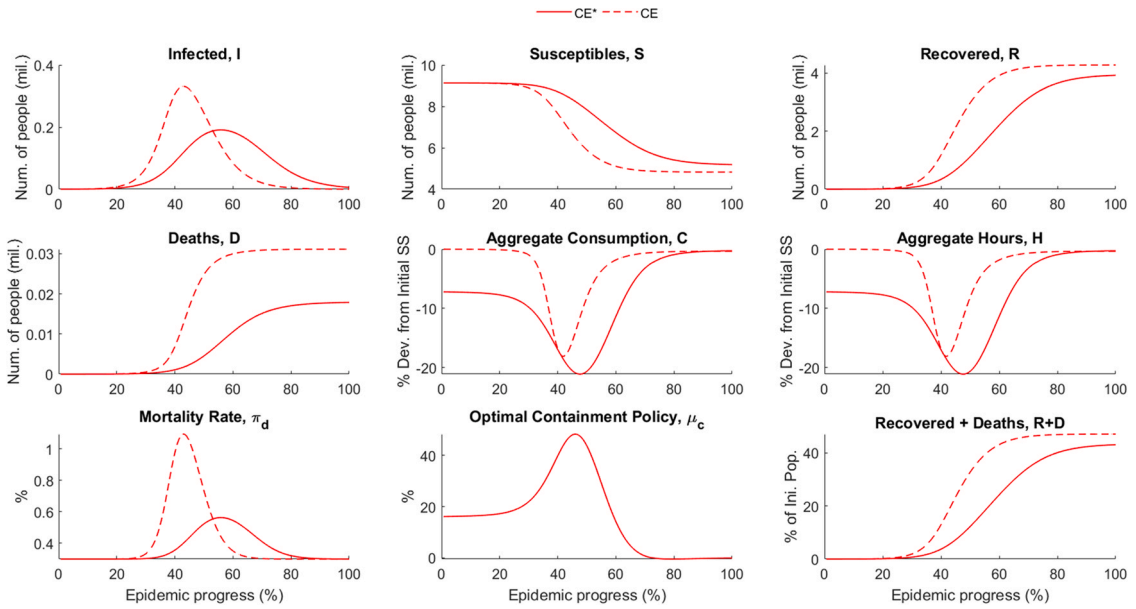

Fig. 9. SIR-macro model – Comparison of results between the scenarios of optimal containment policy (solid line) and competitive equilibrium (dotted lines): Ceará (CE), in level.

Thus, after more than a year,[13] with Brazil as a whole already accumulating approximately 532,000 confirmed deaths and these same states, respectively, 132,000, 13,400, 23,000, 56,600 and 18,100 confirmed deaths, we now compare the preliminary results of the model against real data.[14] For this comparison, we decided to focus on two main variables: cumulative deaths and economic activity.

[13] More accurately, after 1 year, 1 month and 24 days.
[14] The numbers presented in this paragraph are rounded and were collected on July 10, 2021.

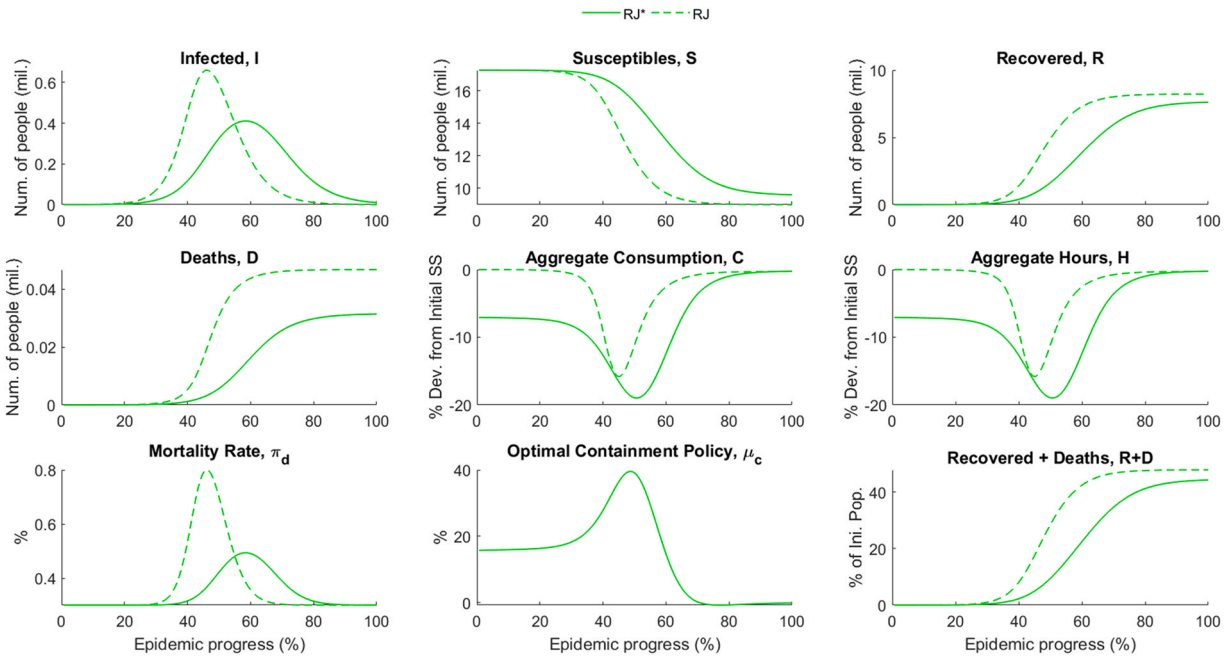

Fig. 10. SIR-macro model – Comparison of results between the scenarios of optimal containment policy (solid line) and competitive equilibrium (dotted lines): Rio de Janeiro (RJ), in level.

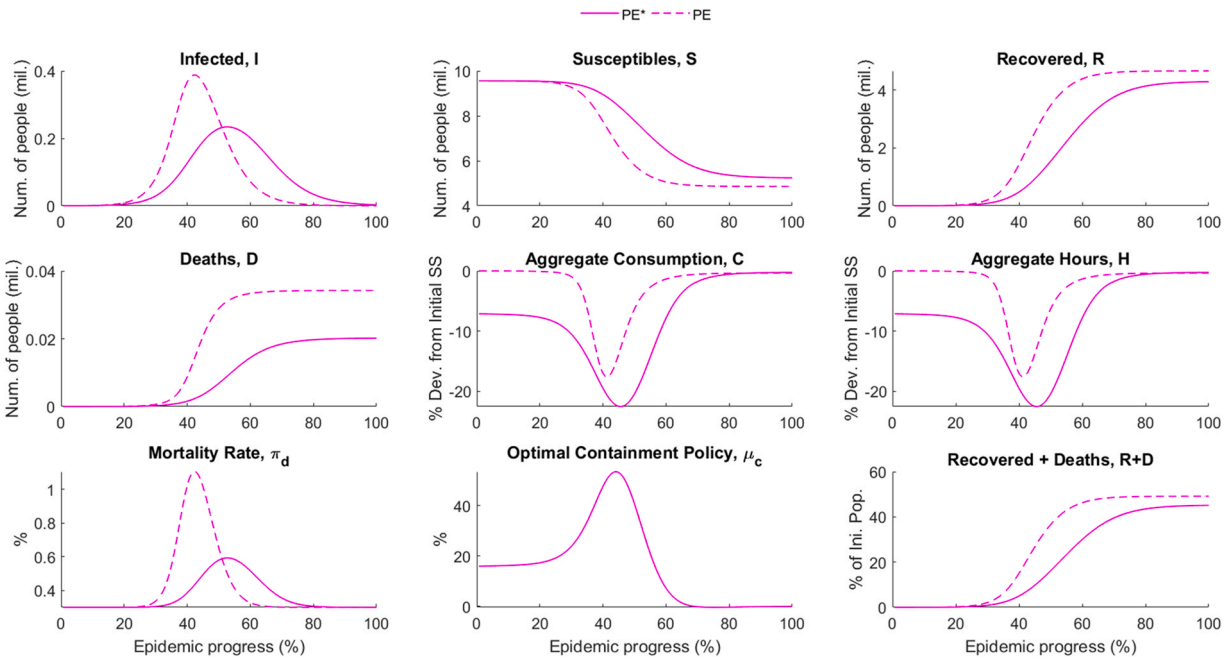

Fig. 11. SIR-macro model – Comparison of results between the scenarios of optimal containment policy (solid line) and competitive equilibrium (dotted lines): Pernambuco (PE), in level.

7.1. One necessary assumption for comparisons

The main challenge to making a proper comparison lies in the fact that we don't know exactly when the 100th infected occurred to suitably fit in time the real data to the model. Model curves start at the time point at which, theoretically, the hundredth *effective* infection occurred. This information, however, is not observable. The most we can observe is the date of the hundredth *notified* infection. But, again, what matters to us is the date of the hundredth *effective* infection. When did it occur?

We are obligated to assume some hypothesis regarding this date. A possible hypothesis (perhaps the simplest) would be the hypothesis that there is no underreporting. Adopting this hypothesis would consist in assuming that the numbers of cases initially notified accurately reflected the infections that actually occurred by COVID-19 at that time. That is, it would consist in assuming that the hundredth *effective* infection actually happened on some date at least very close to the date of the hundredth *notified* infection.

This hypothesis, in our view, is unrealistic. Evidence such as that of Fongaro et al. (2021) suggest that at the time of the hundredth *notified* infection, the degree of underreporting regarding the number of *effective* infections was very large. They find that in November 2019 the COVID-19 virus could already be found in sewers in the state of Santa Catarina (SC). This indicates that even at that time, when there was still no reported case, there were already unreported people infected in Brazil. Therefore, it is reasonable to believe that the 100th *effective* infection by COVID-19 would most likely have occurred a long time ago, relative to the time of occurrence of the 100th *reported* infection.

In an attempt to alleviate this temporal misalignment in the comparison between observed rea-data (notifications) and model data, we then assume a common hypothesis for all states, based on the findings of Fongaro et al. (2021), that the 100th case occurred in November 2019. Therefore, at the starting point of the charts the real observed data starts in November 2019.

7.2. Cumulative deaths

Cumulative deaths data were obtained from the government initiative funded by Brazil's ministry of Health called *Painel Coronavírus*.[15] The comparisons are shown in the Figs. 12-16.

The ideally expected results would be results in which the death curves of the real data lies between the two scenarios evaluated by the model – competitive equilibrium (no policy adoption) and optimal policy adoption –, since the most reasonable to expect would be for the states to adopt a middle ground between these two boundary scenarios. In other words, we would never expect that any state would not adopt any measures, nor that any state would be able to perfectly adopt the optimal trajectory of containment policies prescribed by the model.

As can be seen, the model results in Pernambuco (CE) and Ceará (CE) managed to contain, as expected, the real data in the interval between these two boundary scenarios. Exceptions, however, occurred in three states: Amazonas (AM), São Paulo (SP) and Rio de Janeiro (RJ).

In the case of Amazonas (AM), the healthcare collapse – whose moment of occurrence is indicated by the vertical red dashed line in the graph – could not be predicted by the model, thus reducing the adherence of its results. These results, however, tended to converge to the range predicted by the model at least until before this shock.

In the case of the states of Rio de Janeiro (RJ) and São Paulo (SP), the model also seems to have underestimated what actually happened. Even in the worst-case scenario from a sanitary point of view (competitive equilibrium – no policy adoption) the model predicted fewer deaths than currently reported. Possibly this occurred because, among other reasons, the model was not able to capture the effects of the second wave and new variants, which were very expressive in these states. Notwithstanding, it is possible to notice that before the beginning of the second wave, the trend appeared to be that the accumulated deaths would converge to the interval predicted by the model.

Finally, a problem common to all states' results that is worth noting is that the cumulative deaths expected by the model occur much later than the real data shows. Why did this happen? We identified this time lapse between the predicted and actually observed exponential growth of the pandemic as being caused by a possible structural limitation of the model: when considering a realistic initial number of infected people (one hundred, for example, as is generally assumed by default in epidemiological modeling), the model fails to capture the real dynamics of the temporal evolution of deaths caused by COVID-19.

Eichenbaum et al. (2020) avoided this limitation by taking as the number of people initially infected a percentage of the population that, despite being small in percentage terms, in absolute terms is, in our opinion, very high. He took this number to be $\varepsilon = 0.001$, that is, 0.1% of the pre-epidemic population. In the United States this number would represent an initial infected population of approximately 329,000 Americans.

At the time of the original calibration, comparing this number with then-available data from confirmed cases and making similar comparisons using this percentage for the five selected states, we found the value to be too high and unrealistic. As a result, we preferred to maintain the more realistic hypothesis that in the initial period of the model there were only 100 agents infected in each state.[16]

However, comparing now the results after a year, we realize that this effort to increase the realism of the calibration ended up causing one of the main shortcomings of the model's predictions – that is, these observed time lapses. To better understand how different alternative calibrations of this parameter could have avoided this problem, we performed a sensitivity analysis for

[15] Available at https://covid.saude.gov.br/.

[16] Of course, there is always the possibility that the value we considered at the time of the original calibration to be too high and unrealistic was actually correct. This is something we cannot know, since this quantity, as already discussed, is unobservable. However, we still do not believe this to be the case. At the time of the calibration, we performed several calculation and comparison exercises, including the use of underreporting measures to try to estimate, based on confirmed and reported cases, what could be approximately the actual number of infected people existing at the beginning of the pandemic. For all calculations an ε value of 0.1% seemed too high.

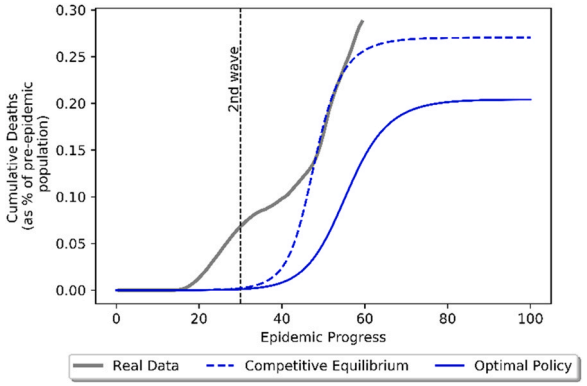

Fig. 12. COVID-19 Cumulative Deaths: São Paulo (SP).

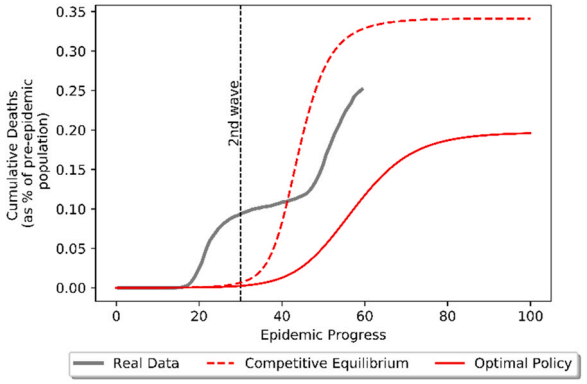

Fig. 13. COVID-19 Cumulative Deaths: Ceará (CE).

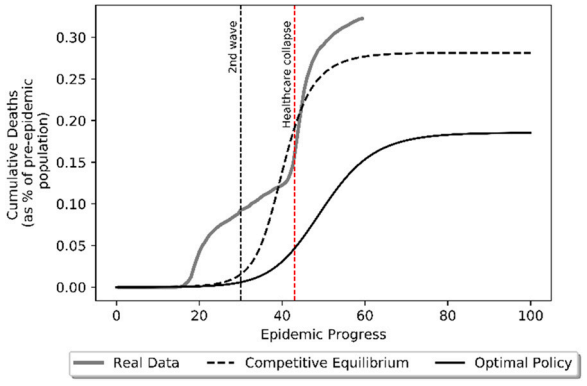

Fig. 14. COVID-19 Cumulative Deaths: Amazonas (AM).

the initial infected population parameter, ε, presented in Appendix A.3. Initially, we also hypothesized that this result could be somehow related to the initial mortality rate for all states, π_d. Therefore, we also performed a sensitivity analysis for this parameter, presented in Appendix A.4.

These two sensitivity analyzes showed that, in fact, the observed time lapse is strongly related to the initial infected population parameter, ε. While variations in the initial mortality rate for all states, π_d, had no temporal shifting effect on the curves, variations in the initial infected population, ε, showed that elevations in this parameter seem to have precisely the pure effect of shifting the macroeconomic and epidemiological curves to the left, while reductions precisely the sheer effect of shifting them to the right, without having any effect on the levels of peaks, final cumulative deaths, or depths of recessions. This shows that the observed time lapse problem could have been avoided without affecting any other result of the model, simply by adopting a higher – albeit possibly unrealistic – value for the initial infected population. – exactly what was done by Eichenbaum et al. (2020).

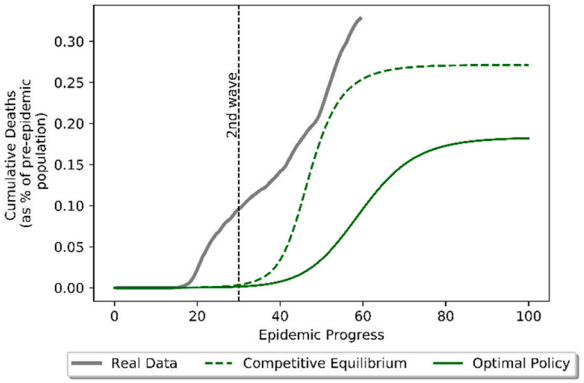

Fig. 15. COVID-19 Cumulative Deaths: Rio de Janeiro (RJ).

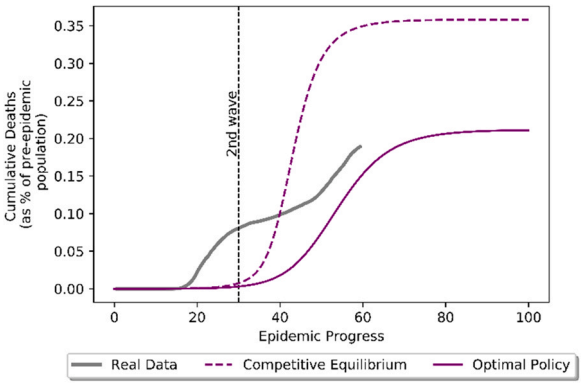

Fig. 16. COVID-19 Cumulative Deaths: Pernambuco (PE).

7.3. Economic activity

Regarding economic activity, the first-order prediction of the model for the five states analyzed was that, in response to the regional epidemics, the activity would undergo a sharp contraction followed by a robust recovery. This *qualitative* prediction is clearly supported by data for the five Brazilian states considered. Surprisingly, despite its simplicity, the model also did reasonably well at capturing the broad *quantitative* decline in the states' economic activity.

This can be easily verified comparing the peak-to-trough decline in economic activity predicted by the model against the peak-to-trough decline in the Regional Economic Activity Index (IBCR)[17] of the five modeled states. These numbers are presented in Table 6.

Peak-to-trough decline in the real data (IBCR) was calculated considering the decline between November 2019 – the date that, as already discussed, we assumed epidemics started – and April 2020, the month in which the trough of economic activity took place in the five states.

As can be seen, in all the states considered, with the exception of Amazonas (AM) and Rio de Janeiro (RJ), the drop in economic activity observed in real data through the IBCR is contained within the decline interval predicted by the two boundary scenarios computed by the model.

Not only were these quantitative predictions remarkably accurate for most states: the conclusions about the relative interstate economic impact were also reasonably correct from a qualitative point of view.

The model predicted that the state that would suffer the least potential recession as a result of the epidemic would be the state of Rio de Janeiro (RJ). Real data show that, in fact, the state of Rio de Janeiro (RJ) was the one that suffered the smallest decline in economic activity. The state that would suffer the second smallest potential recession would be the state of São Paulo (SP), a position that was also confirmed by real data.

Furthermore, the model predicted that the state that would suffer the greatest potential recession as a result of the epidemic would be the state of Pernambuco (PE). Real data show that, of the five states analyzed, Pernambuco (PE) was the second most impacted state, just behind the idiosyncratic state of Amazonas (AM).

[17] Data obtained from the Central Bank of Brazil's time series management system – *Sistema Gerenciador de Séries Temporais* (SGS).

Table 6
Peak-to-trough decline in economic activity: model versus real data (IBCR).

	Scenario	SP	AM	CE	RJ	PE
Model	**Competitive Eq.**	-13.55%	-13.67%	-18.11%	-15.80%	-17.66%
	Optimal Policy	-19.28%	-19.72%	-21.10%	-18.98%	-22.58%
Real data (IBCR)		-16.30%	-27.16%	-19.48%	-11.60%	-20.71%

While providing a detailed comparison of model results and data (e.g. plotting the overlay comparison of actual data recession curves in conjunction with model recession curves) would require data at frequencies that unfortunately are not available, we can still give a step beyond the broad statements made so far by plotting actual recession curves in isolation.[18] This will allow us to qualitatively assess, for example, some other aspects such as the speed of recovery between states after the valley and possible second waves of recession. The actual data recession curves are shown in Fig. 17.

First, it is interesting to note how, in regional terms, the movements of the economies observed in the real data were uneven and how this may be reflecting elements such as, in some cases, distinct productive structures, while, in others, differences in the increase in mobility. As an example of these phenomena, we can analyze the two states for which the model failed to contain the observed recession within the range of considered scenarios: Rio de Janeiro (RJ) and Amazonas (AM).

As pointed out in a report published by Firjan,[19] in the case of Rio de Janeiro the smaller fall in the economy, compared to other states in the country, was mainly justified by the performance of the extractive industry. While the other large sectors reduced production in the period, despite the health crisis, the oil and gas sector showed high growth (+14.5%), driven by the increase in oil exports, offsetting the reduction in domestic demand for fuel.

In the case of Amazonas, the July 2020 Regional Bulletin published by the Central Bank of Brazil[20] points out that the reduction in the retail was more accentuated than that observed in the country's average, largely reflecting the intense social isolation in the region. Moreover, data from the Brazilian Institute of Geography and Statistics (IBGE) show that the sectoral composition of the Amazonas industry contributed to an even worse result in this state. In April 2020, the industrial production of Amazonas contracted 53.9%, compared to the same period of the previous year. Amazon was in the last position among the states. And the best ones were: Pará with 37.6%, Goiás with 0.4% and Rio de Janeiro with − 5.4%.[21]

These numbers show the size of the potential importance of sectoral compositions in determining the states' macroeconomic reactions to the pandemic and show that one of the possible reasons for the failure to predict the magnitude of recessions in the states of Rio de Janeiro (RJ) and Amazonas (AM) by the model may lie precisely in its inability to capture these distinct productive structures.

Therefore, a possible and interesting extension of the model would be the consideration of these distinct productive structures. With this consideration, perhaps the model would better capture, for example, in the case of Rio de Janeiro, the above-average performance of the extractive industry and, in the case of Amazonas, the below-average performance of the retail sector and industrial production. This could potentially resolve the shortcomings observed in the macroeconomic predictions obtained for these states using the basic SIR-macro model.

An extension along the lines of what is done by Krueger et al. (2020), for example, could solve the problem. They extend the previous theoretical framework of Eichenbaum et al. (2020) assuming an economy composed of several heterogeneous sectors that differ in technology and infection probabilities. The authors found that a model with heterogeneous agents produces a different economic outcome. In detail, they demonstrate it is possible to mitigate the economic and human costs of the COVID-19 crisis without government intervention and allowing agents to shift their sectoral behavior. Moreover, since the transmission rate is not the same across sectors, if the model allows for more sectors the government could reduce the spread of the disease by allocating consumers to low-infectious sectors.[22]

Another interesting phenomenon that can be noticed in the data is the apparent beginning, at the end of the considered period, of second waves of recession, especially sharper in less developed states such as Amazonas (AM), Ceará (CE) and Pernambuco (PE). These second waves may be strongly related to new variants that enable or reinforce the occurrence of reinfections. Extensions of the epidemiological framework of the model to allow the occurrence of multiple strains – e.g., the so-

[18] The problem is that we only have the IBCR data in quarterly frequency. This leaves us with only 18 observations regarding economic activity for the period considered. To plot comparisons similar to those presented in the previous section for cumulative deaths, we would need data at higher frequency. A forced solution would be to interpolate the data to enable comparison. However, in our view, data transformations of this nature would excessively distort the series, making them unsuitable for comparison.

[19] *Rio de Janeiro: Resultados e perspectivas para o PIB – 3º trimestre 2020 e projeções*, technical report available at: https://www.firjan.com.br/publicacoes/publicacoes-de-economia/pib-brasil-e-rio-de-janeiro-resultados-e-projecoes.htm.

[20] *Boletim Regional do Banco Central do Brasil*, volume 14, number 3. July 2020. Available at: https://www.bcb.gov.br/publicacoes/boletimregional/202007.

[21] *"Produção industrial do AM cai mais de 50% e registra piores resultados do País no mês de abril, aponta IBGE"*, G1 AM, 09/06/2020. Available at: https://g1.globo.com/am/amazonas/noticia/2020/06/09/producao-industrial-do-am-cai-mais-de-50%-e-registra-piores-resultados-do-pais-no-mes-de-abril-aponta-ibge.ghtml.

[22] Our sincere thanks, especially here, to the anonymous reviewer whose comments and suggestions helped to significantly improve and clarify this section. We really enjoyed the proposed discussions on the cases of Amazonas (AM) and Rio de Janeiro (RJ), as well as the discussion on the article by Krueger et al. (2020).

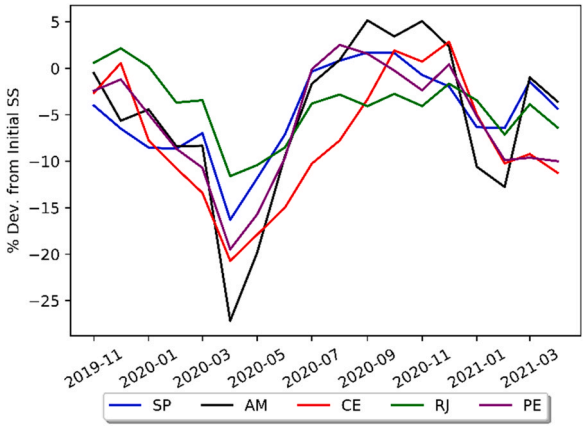

Fig. 17. Real data recession curves for all states – IBCR cumulative variation as of November 2019.

called multi-strain SIR models such as the one proposed by Arruda et al. (2021) – could contribute to the results being able to capture these multiple recessive waves.

In sub-regional context, coordination failures between state and federal governments can also be the reason for this phenomenon. Góes and Borelli (2021), for example, consider this possibility by modeling uncoordinated scenarios. They find, as one of the results, precisely two recessive waves, which are also more accentuated in less developed states. The authors argue that, given the possibility of delays in carrying out containment measures in an uncoordinated scenario, the peak of the containment rate may occur later than the moment of occurrence of the peak of infected population. Thus, at certain times, while the infected population declines, the containment rate increases and, from a macroeconomic point of view, two effects in opposite directions occur simultaneously: while the reduction of the infected population acts by boosting economic activity, the increasing containment rate obviously acts by reducing it.

In these moments, the consequence on macroeconomic aggregates is ambiguous and depends on the magnitude of the two effects that act simultaneously. If the recessive effect of the increase in the containment rate on economic activity outweighs the effect of the resumption of the flow of recovered people returning to consumption and work, the lack of coordination causes a second recessive movement to start, which only ends with the beginning subsequent flexibility of containment measures. Therefore, such an extension of the model for the possibility of uncoordinated measures to combat the pandemic would also be interesting and could allow results to capture the presence of multiple recessionary economic waves.

7.4. Final remarks

The model proved capable of predicting both cumulative deaths and declines in states economic activities with reasonable consistency. In the case of cumulative deaths, although the model has quantitatively underestimated the deaths resulting from the pandemic in some states, it still presented qualitatively acceptable predictions. In the case of economic activity, the results were both qualitatively and – except for the state of Amazonas (AM) and Rio de Janeiro (RJ) – quantitatively precise.

It is important to keep in mind that the original calibrated model doesn't considered the possibility of re-infections, new strains, and/or multiple waves. These results should be evaluated in light of the time and context in which they were obtained: the calibration was done at the beginning of the pandemic, in May 2020, when uncertainty about the nature of the virus was at its height.

The fact is that, despite the simplicity of the model and the scarcity of data (mainly microdata) for calibration and all the uncertainty regarding the nature of the virus at the beginning of the pandemic, the predictions, at least from a qualitative point of view, are demonstrated reasonably acceptable. Evidently, due to its structural limitations, the model was unable to capture the exact dynamics of the real-data. Indeed, even Eichenbaum et al. (2020) itself assumed that one of the limitations of the model was its inability to correctly simulate the timing of some events under certain circumstances.[23]

It is also important to emphasize that the recent literature based on the basic SIR-macro model has some shortcomings. Some of its straightforward limitations, as already discussed, are not considering the possibility of new strains/variants and/or multiple waves, as well as not considering the possibility of different productive structures. In the sub-regional context, not considering the possibility of lack of coordination between state and federal governments – at least in the way as we consider the modeling of states here – is also a shortcoming, especially for the Brazilian case.

Furthermore, despite having the interesting feature of being able to endogenize macroeconomic responses to epidemiological conditions, the model still lacks to be highly stylized, based on many simplifying assumptions – e.g. a uniform and

[23] See Eichenbaum et al. (2021), p. 34.

constant contact rate between susceptible and infected populations – which are clearly violated in practice. The model does not incorporate detailed information about social interactions and demographics at micro-geographical levels, which is something that is done in state-of-the-art epidemic models, making them somewhat more realistic (e.g. Ferguson et al., 2020 and Acemoğlu et al., 2020).

These more realistic models, however, also have their limitations from the economic point of view. They have not yet been incorporated into a coherent economic framework – such as that offered by the SIR-macro model – capable of informing potential trade-offs between public health and economic activity. Therefore, the integration of these features could be an important and interesting extension still available for new research agendas.

Despite these shortcomings, we believe that, for the purpose of predicting *ex-ante* the potential severity of the pandemic at a time of extreme uncertainty, the results proved to be quite useful and sufficient for the authorities, if they so wished, to anticipate the need for active policies of combating the pandemic. As discussed in greater detail above, these results could have been even better given the implementation of some of the aforementioned extensions to the model to address the shortcomings discussed, as well as if the model had been continually recalibrated throughout the pandemic in view of new data availability.

8. Conclusion

Our interest was to analyze qualitatively how the main intrinsic differences of each state could affect its epidemic dynamics and results. In particular, our exercises carried out for five states selected by the severity of the epidemic they presented at the time of the research, pointed to substantial potential differences in the evolution and outcome of the epidemic in each state, both in the competitive equilibrium scenario and in the scenario in which optimal containment policies are adopted.

In both scenarios, we found evidence of potential differences in i) the size of the infected population peak, ii) the time required to reach the infected population peak, iii) the depth of the recessions, iv) the duration of the recessions, v) the share of the initial population that has been infected by the end of the epidemic and vi) the share of the initial population that died by the end of the epidemic in each state.

The results presented showed that the intrinsic differences of each state could also imply different optimal trajectories of containment policies for each one of them. These intrinsic differences could affect i) the initial severity of the containment measures that ideally should be adopted by each state, as well as the dynamics of the evolution of these containment rates over time, implying ii) differences in the ideal moment that the containment measures would need to be elevated, iii) to what extent they would need to be elevated, and iv) when they could finally be relaxed.

Using the simple framework of the SIR-macro model proposed by Eichenbaum et al. (2020) and analyzing the results obtained for each state, we conclude that the main implicit characteristics of the five different states could imply relevant differences in

i) the epidemic dynamics and its general epidemiological consequences;
ii) the optimal containment policies to be adopted by each state;
iii) the effect of adopting optimal containment policies;
iv) the severity of the economic recessions from the epidemic.

This conclusion emphasized the importance of a disaggregated analysis of countries with huge geographic and demographic dimensions – such as Brazil – in the formulation of coordinated policies to combat COVID-19.

At the time of the first draft of the paper, we warned that the adoption of single centralized and aggregated policies for huge and heterogeneous countries like Brazil could trigger a series of containment policy errors across the country's states and regions, deepening both the economic recession and the number of deaths resulting from the epidemic. In the presence of a large heterogeneity in the optimal level of containment policy required for each state, a single containment policy for the whole country would be unable to adequately deal with the needs of all states simultaneously. Inevitably, the containment rate adopted across the country would be lower than needed for some states, resulting in more deaths, and higher than needed for others, resulting in unnecessarily in deeper economic recessions.

Approximately one year after the original *ex-ante* calibration, we evaluated the predictions made by the model comparing it to *ex-post* real-world data. The results of the model showed to be reasonably consistent, at least qualitatively, when considering the simplicity of the model and the context and the time when it was calibrated – surrounded by uncertainty about the nature of the virus and by the scarcity of data to calibrate the model in a more precise way.

We conclude that, in times and circumstances of emergency, the model results could have been used to qualitatively anticipate the potential tragedy of the pandemic that later materialized in Brazil, being sufficient for the authorities, if they so wished, to derive from it active policy lessons for combating the pandemic. Of course, as discussed, the results could have been even better if the model had been continually recalibrated throughout the pandemic in view of new data availability, as well as with the implementation of some of the previously mentioned extensions. The consideration of, e.g., distinct productive structures, multiple strains, incoordination between states and federation and detailed information about social interactions and demographics at micro-geographical levels to the model could address the shortcomings discussed, setting up a promising future research agenda.

Appendix A. Sensitivity analysis

In this appendix we present sensitivity analyzes for the parameters regarding i) the share of transmissions that occur at work, α_2, ii) the share of transmissions that occur in other activities, α_3, iii) the initial infected population, ε, and the iv) initial mortality rate, π_d.

Since computing optimal policy equilibrium is computationally cumbersome[24] and, in terms of comparative dynamics, the sensitivity analysis results for this scenario would be qualitatively very similar to sensitivity analyzes for the competitive equilibrium scenario, we decided, for the sake of simplicity, to perform all analyzes only for the competitive equilibrium scenario. Results for this scenario were sufficient to illustrate how the model results would react to alternative calibrations and saved us from incurring a very high computational cost for a very low return.

For the share of transmissions that occur at work (α_2), the alternative calibration values used in analysis were chosen so as to cover the entire range of possible values that such parameter could assume, keeping the share of transmissions that occur in other activities (α_3) fixed and the share of transmissions that occur in consumption (α_1) residually calculated.[25] In addition to the results of the original calibrated model, we present computed results for four other alternative values, uniformly distributed in this range. The alternative values of α_3 were chosen following the same logic, but keeping the parameter α_2 fixed.

For the initial infected population (ε), we present, in addition to the results using the original calibration, results computed for the model using the value assumed by Eichenbaum et al. (2020), that is, $\varepsilon = 0.001$. Just for the sake of comparison, in order to allow a better understanding of the possible consequences of different alternative calibrations for this parameter, we also present results considering three other smaller alternative values, obtained simply by successively dividing by 4 the value used by Eichenbaum et al. (2020).

Finally, for the alternative values of π_d we select a range of values that we deem feasible and sufficient to provide an adequate comparison and a good sense of the possible consequences of alternative calibrations for this parameter.

The results of all these sensitivity analyses, for all five states considered, are presented on the next pages.

A.1. Share of transmissions that occur at work (α_2)

see Figs. 18–22.

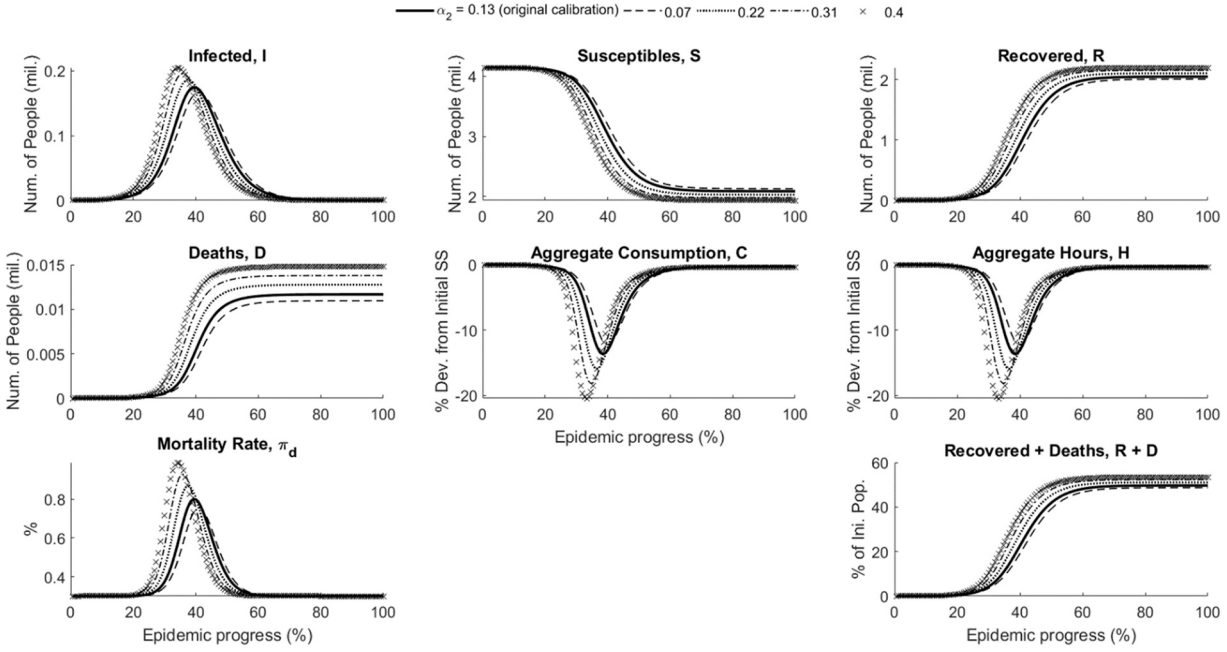

Fig. 18. Sensitivity analysis of α_2 (holding α_3 fixed and α_1 residually calculated) for Amazonas (AM) in competitive equilibrium scenario.

[24] Computing optimal policy equilibria is very computationally cumbersome. Each equilibrium in this scenario takes around 5 h to compute, using a 7th generation Intel Core i7 processor. In view of this, computing four alternative calibration scenarios for each of the five states in the optimal policy scenario has become very costly relative to the few benefits it would present.

[25] Remember that, by definition, $\alpha_1 + \alpha_2 + \alpha_3 = 1$.

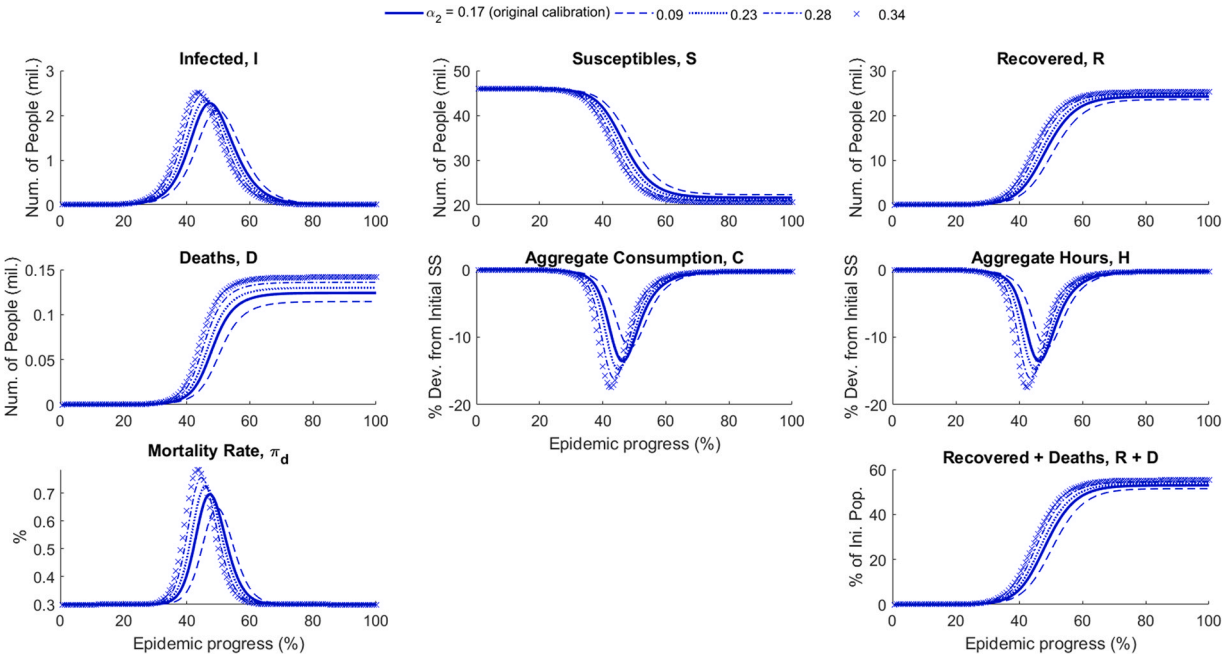

Fig. 19. Sensitivity analysis of α_2 (holding α_3 fixed and α_1 residually calculated) for São Paulo (SP) in competitive equilibrium scenario.

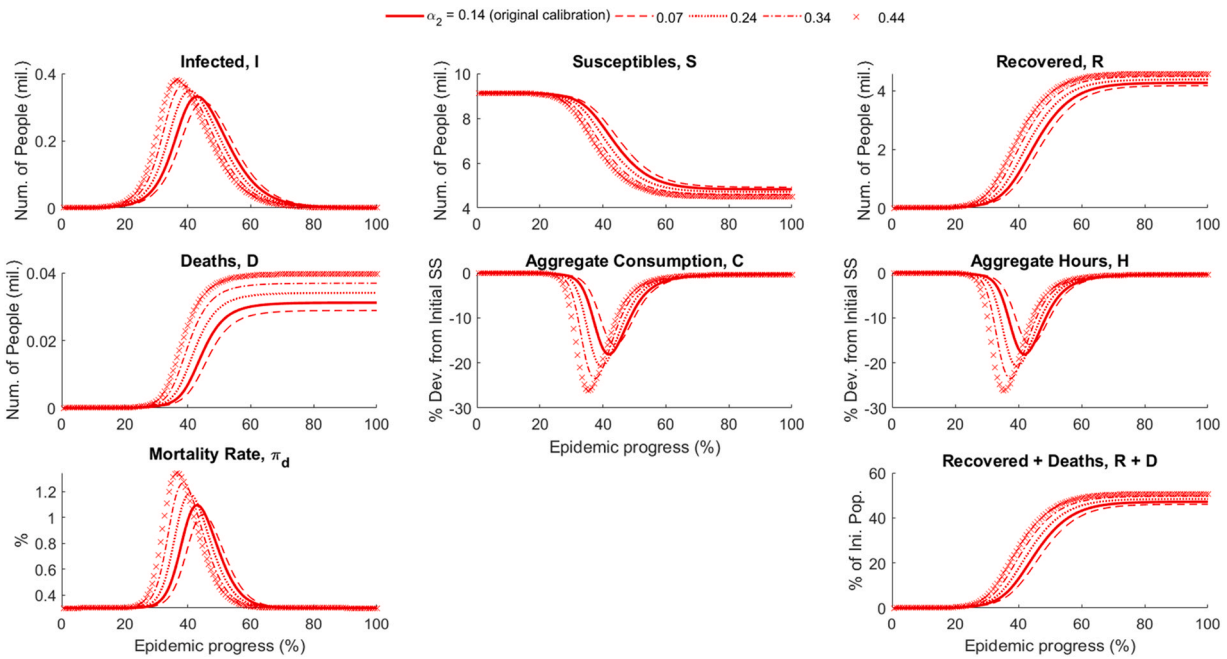

Fig. 20. Sensitivity analysis of α_2 (holding α_3 fixed and α_1 residually calculated) for Ceará (CE) in competitive equilibrium scenario.

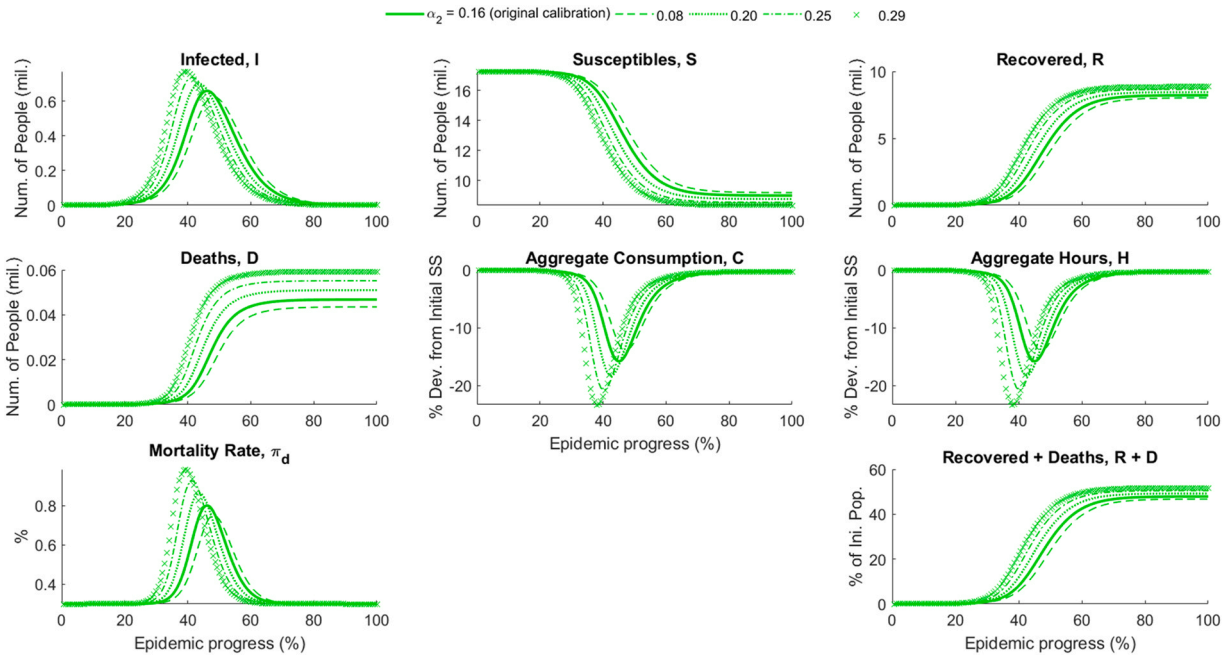

Fig. 21. Sensitivity analysis of α_2 (holding α_3 fixed and α_1 residually calculated) for Rio de Janeiro (RJ) in competitive equilibrium scenario.

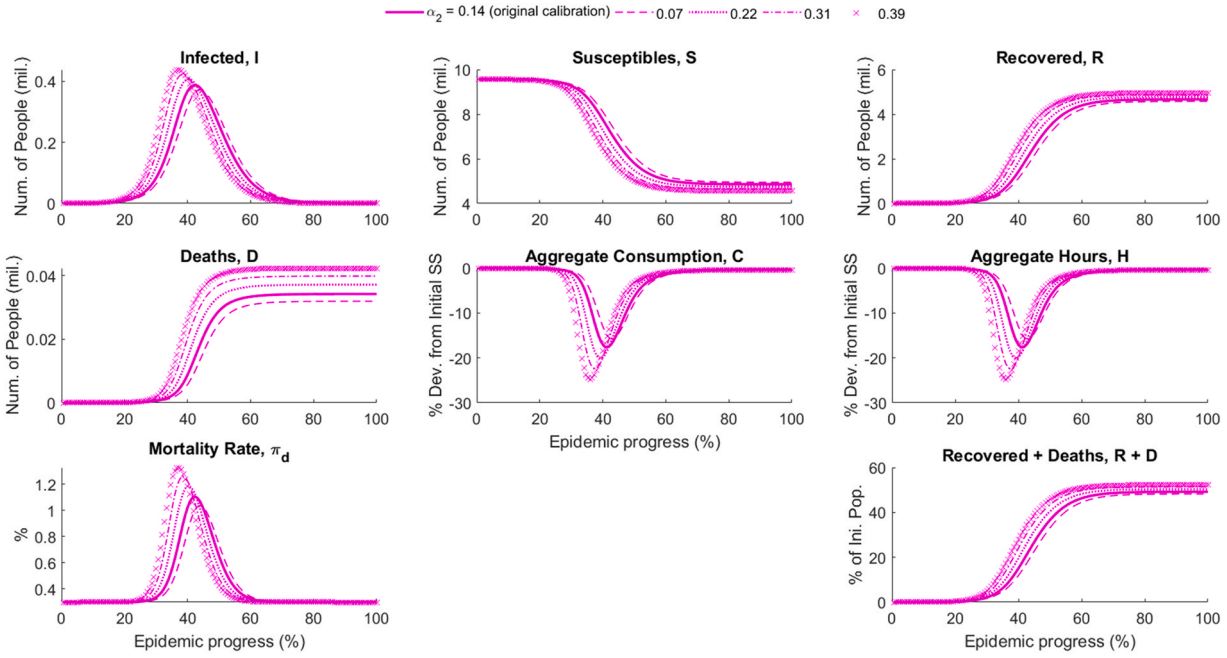

Fig. 22. Sensitivity analysis of α_2 (holding α_3 fixed and α_1 residually calculated) for Pernambuco (PE) in competitive equilibrium scenario.

A.2. Share of transmissions that occur in other activities (α_3).

see Figs. 23–27.

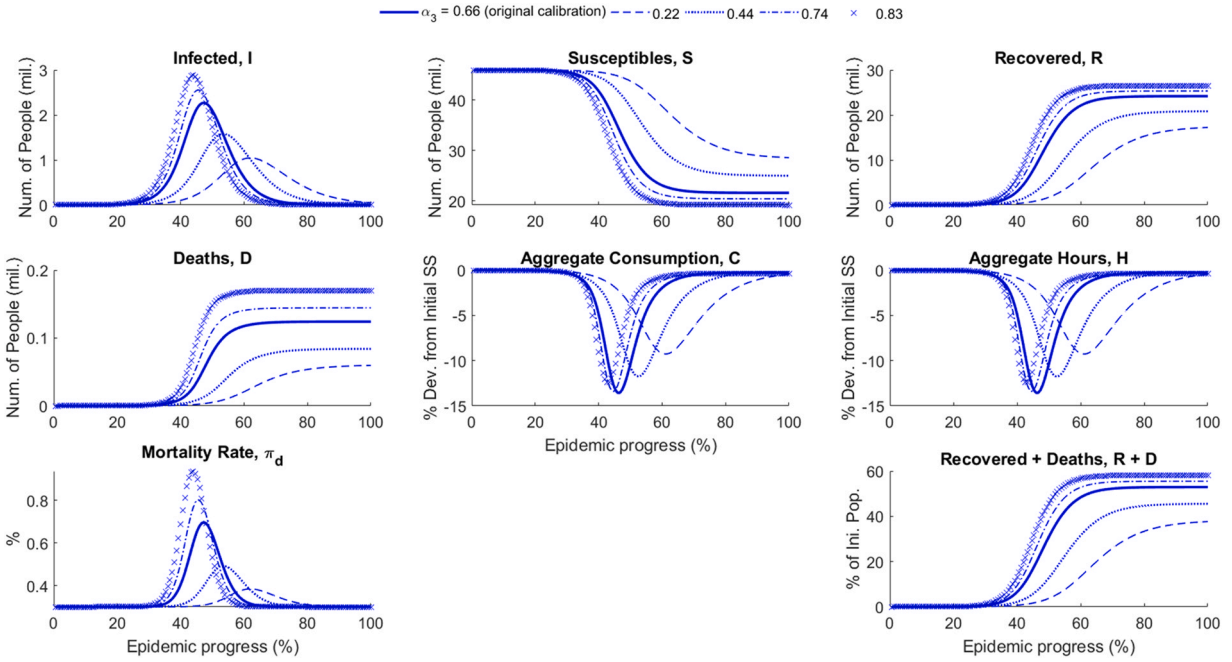

Fig. 23. Sensitivity analysis of α_3 (holding α_2 fixed and α_1 residually calculated) for São Paulo (SP) in competitive equilibrium scenario.

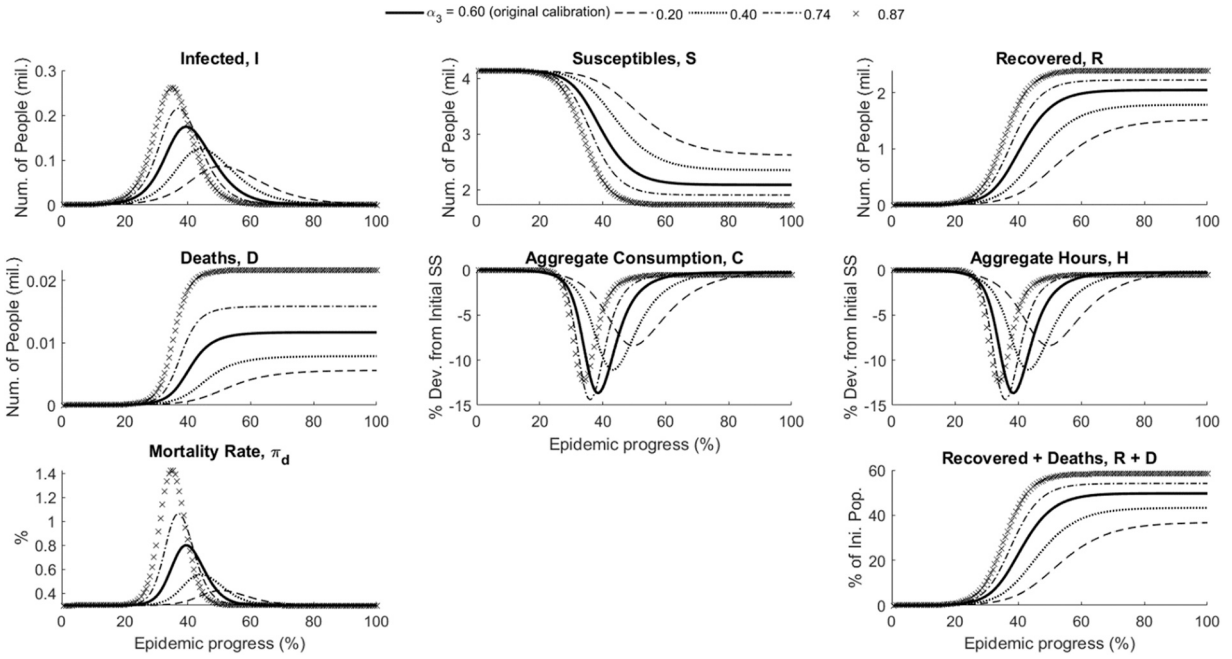

Fig. 24. Sensitivity analysis of α_3 (holding α_2 fixed and α_1 residually calculated) for Amazonas (AM) in competitive equilibrium scenario.

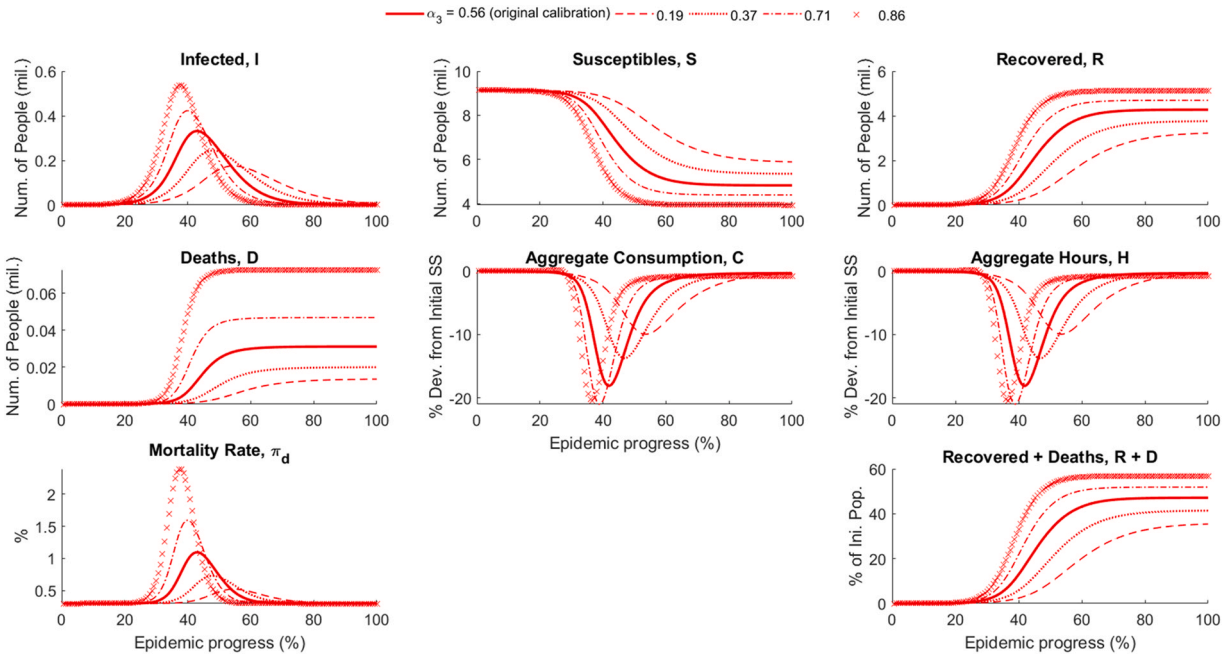

Fig. 25. Sensitivity analysis of α3 (holding α2 fixed and α1 residually calculated) for Ceará (CE) in competitive equilibrium scenario.

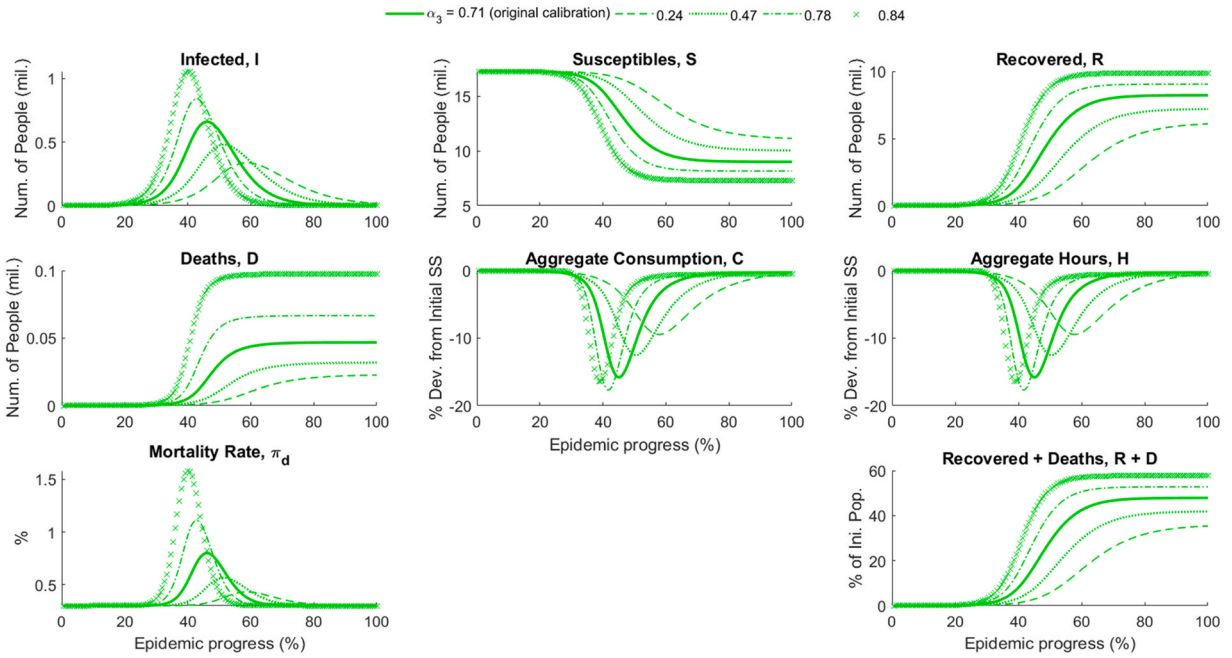

Fig. 26. Sensitivity analysis of α_3 (holding α_2 fixed and α_1 residually calculated) for Rio de Janeiro (RJ) in competitive equilibrium scenario.

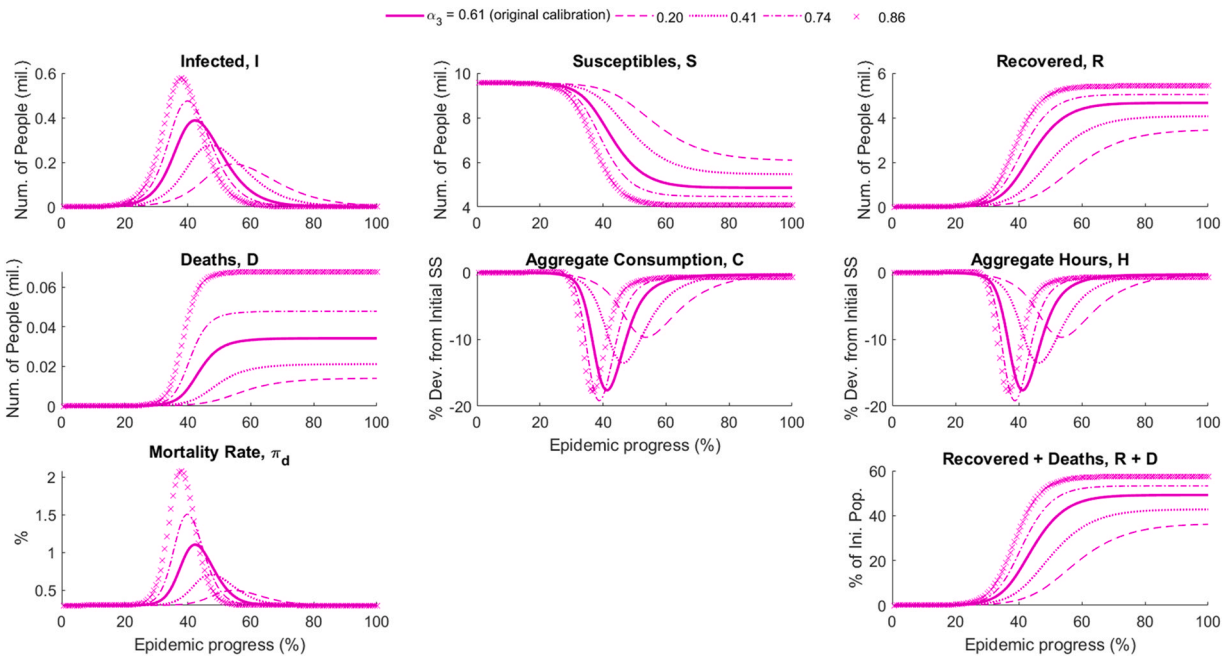

Fig. 27. Sensitivity analysis of α3 (holding α2 fixed and α1 residually calculated) for Pernambuco (PE) in competitive equilibrium scenario.Initial infected population (ε).

A.3. Initial infected population (ε)

see Figs. 28–32.

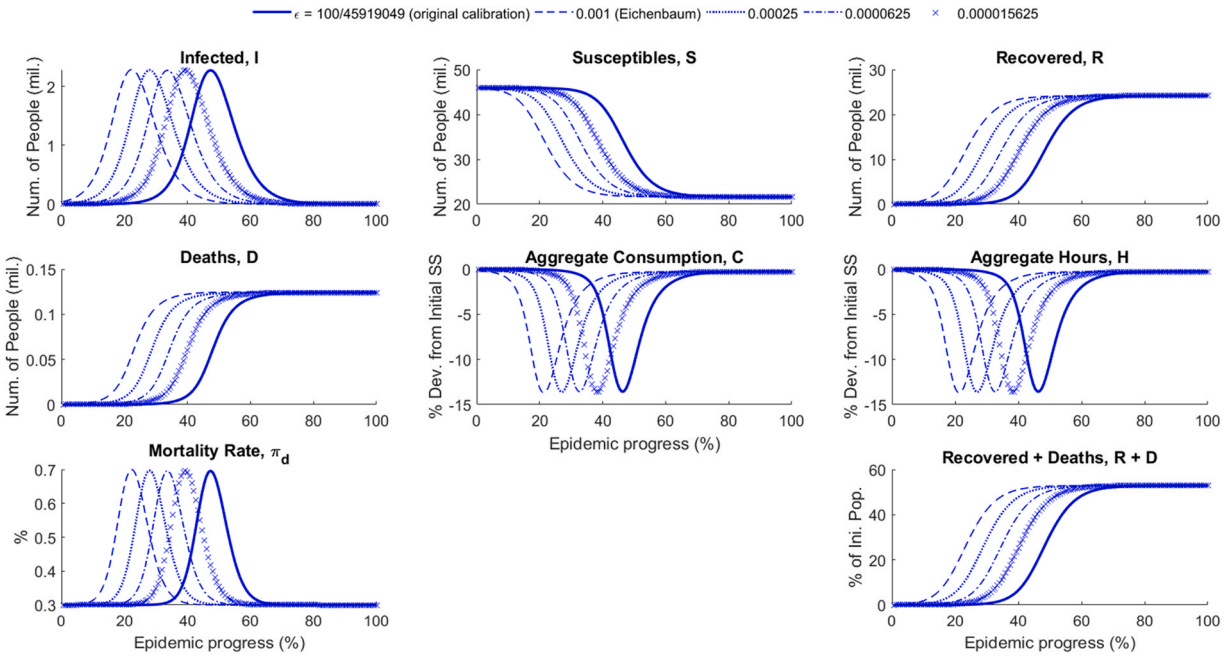

Fig. 28. Sensitivity analysis of initial infected population, ε, for São Paulo (SP) in competitive equilibrium scenario.

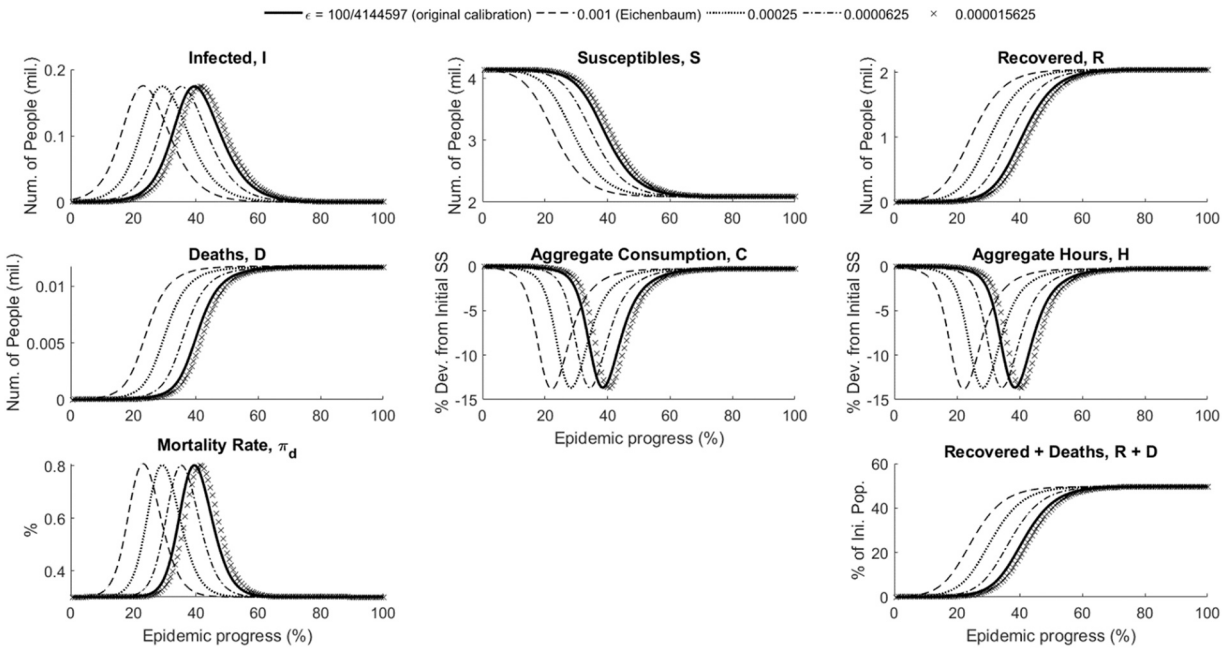

Fig. 29. Sensitivity analysis of initial infected population, ε, for Amazonas (AM) in competitive equilibrium scenario.

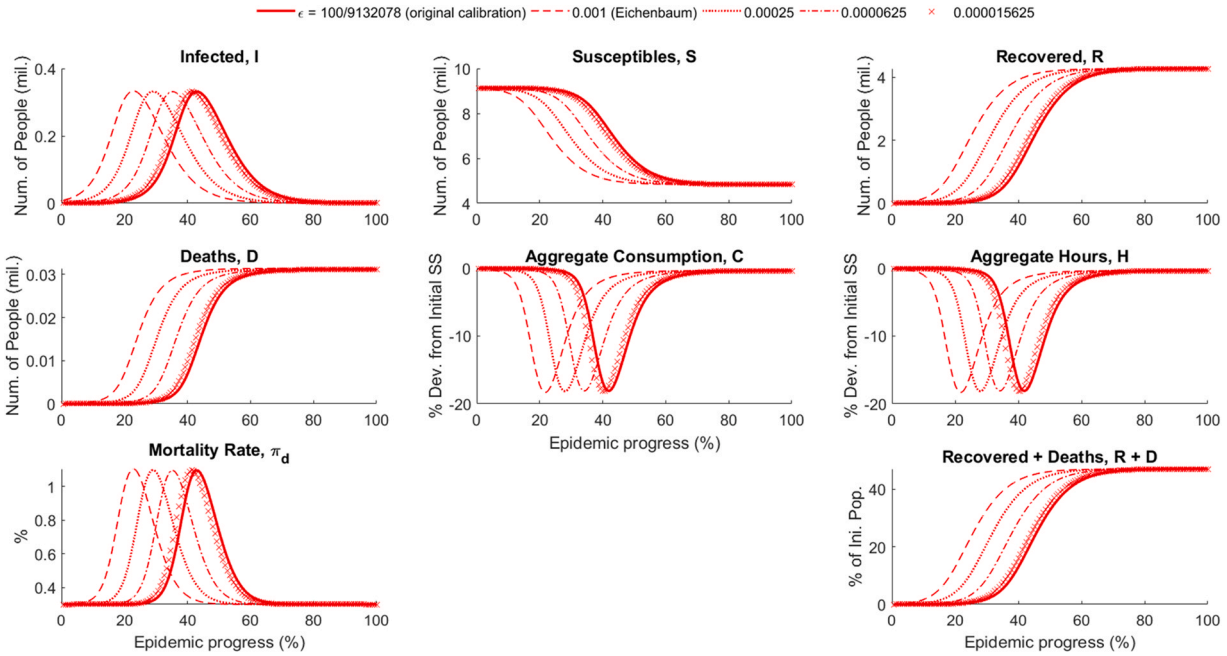

Fig. 30. Sensitivity analysis of initial infected population, ε, for Ceará (CE) in competitive equilibrium scenario.

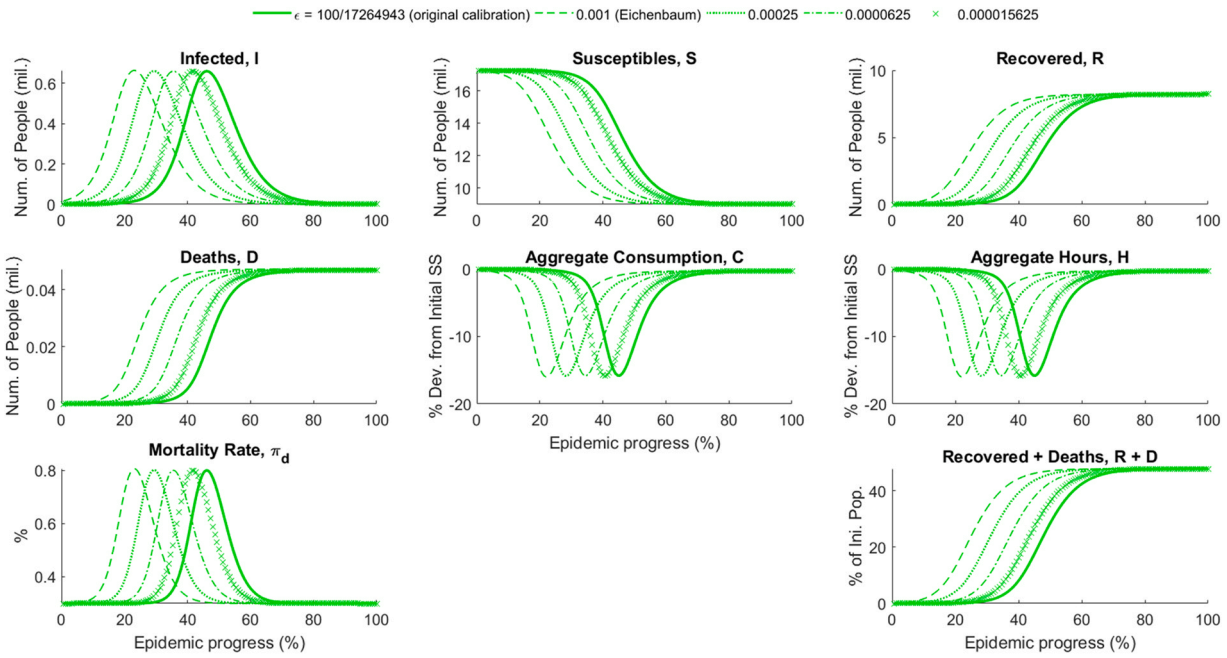

Fig. 31. Sensitivity analysis of initial infected population, ε, for Rio de Janeiro (RJ) in competitive equilibrium scenario.

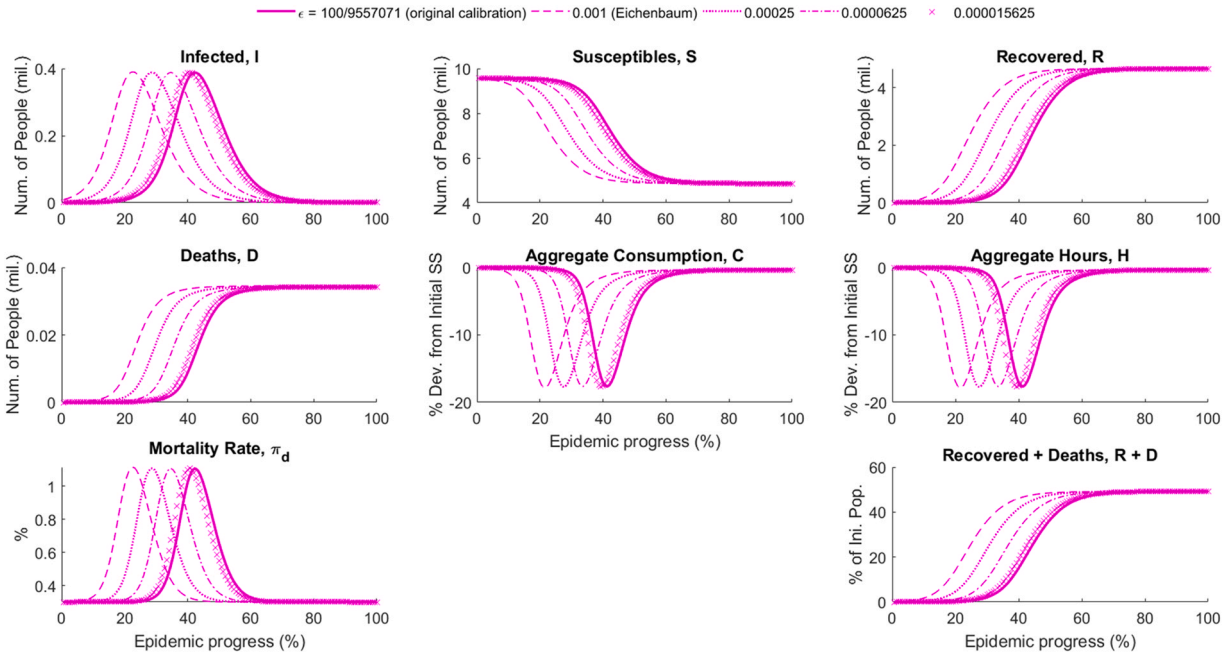

Fig. 32. Sensitivity analysis of initial infected population, ε, for Pernambuco (PE) in competitive equilibrium scenario.

A.4. Initial mortality rate (π_d)

see Figs. 33–37.

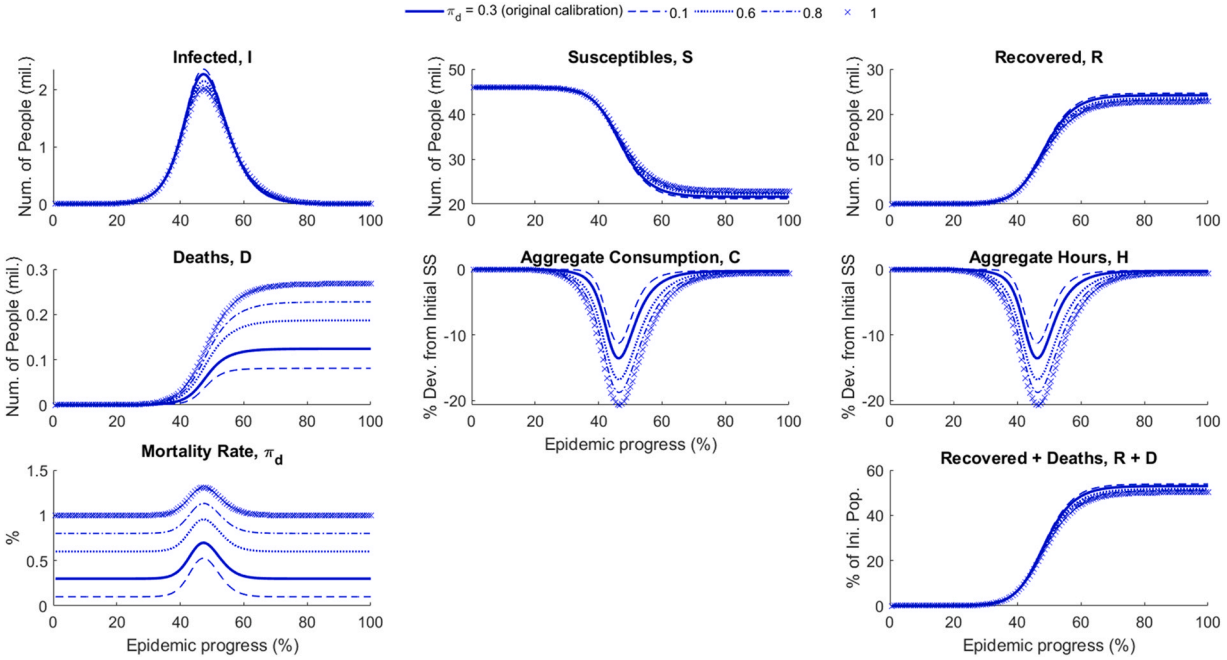

Fig. 33. Sensitivity analysis of initial mortality rate, π_d for São Paulo (SP) in competitive equilibrium scenario.

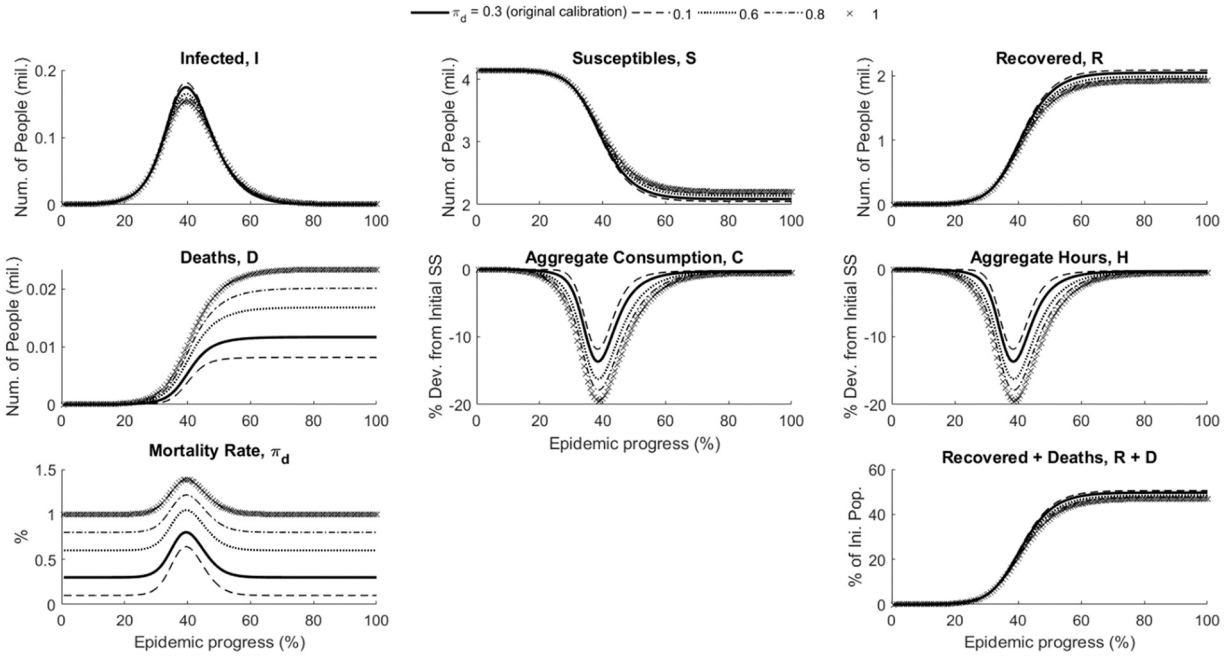

Fig. 34. Sensitivity analysis of initial mortality rate, π_d, for Amazonas (AM) in competitive equilibrium scenario.

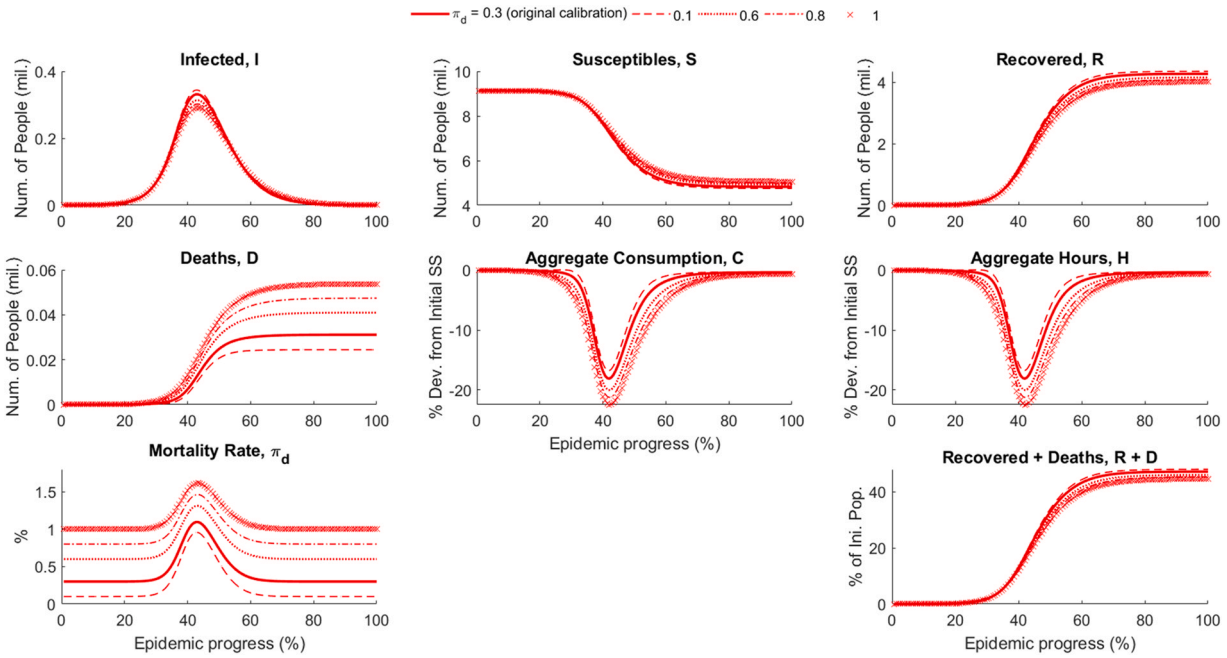

Fig. 35. Sensitivity analysis of initial mortality rate, π_d, for Ceará (CE) in competitive equilibrium scenario.

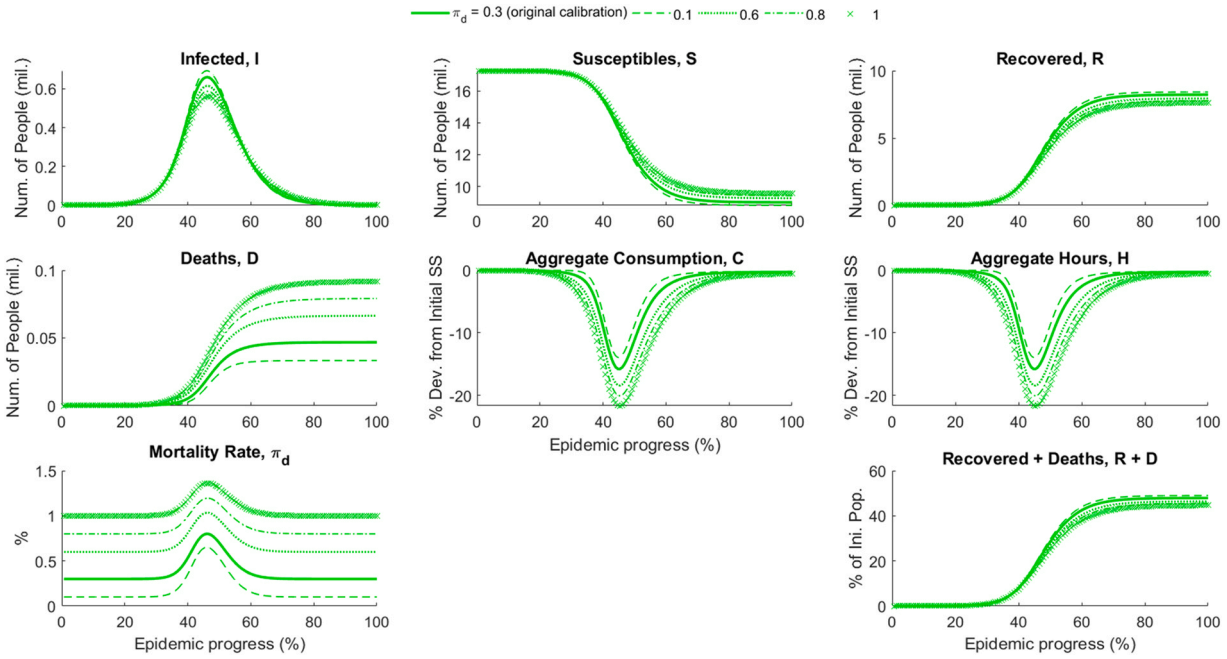

Fig. 36. Sensitivity analysis of initial mortality rate, π_d, for Rio de Janeiro (RJ) in competitive equilibrium scenario.

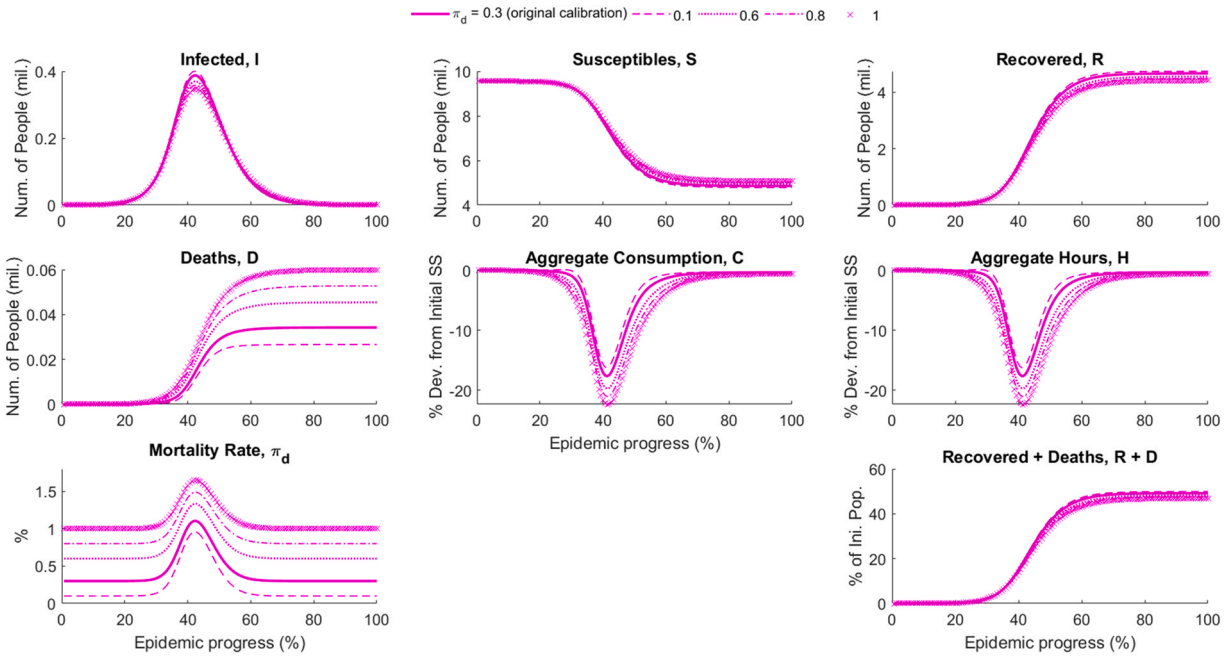

Fig. 37. Sensitivity analysis of initial mortality rate, π_d, for Pernambuco (PE) in competitive equilibrium scenario.

References

Acemoğlu, D., Chernozhukov, V., Werning, I., Whinston, M., 2020. A Multi-risk SIR Model with Optimally Targeted Lockdown. NBER Working Papers, No. 27102.

Arruda, E.F., Das, S.S., Dias, C.M., Pastore, D.H., 2021. Modelling and optimal control of multi strain epidemics, with application to COVID-19. PLoS One 16, 9.

Bastos, S.N., Cajueiro, D.O., 2020. Modelling and forecasting the early evolution of the Covid-19 pandemic in Brazil. Sci. Rep. 10 article #19457.

Boianovsky, M., 2021. Economists, scientific communities, and pandemics: an exploratory study of Brazil (1918–2020). EconomiA 22, 1–18.

Borelli, L., Góes, Geraldo S., 2020a. Macroeconomics of epidemics: interstate heterogeneity in Brazil. Covid Economics: Vetted and Real-Time Papers. 30. pp. 83–119.

Borelli, L., Góes, Geraldo S., 2020b. A Macroeconomia das Epidemias: Heterogeneidade Interestadual no Brasil. Texto para Discussão IPEA No. 2581.

Campos, E.L., Cysne, R.P., Madureira, A.L., Mendes, G.L.Q., 2021. Multi-generational SIR modeling: determination of parameters, epidemiological forecasting and age-dependent vaccination policies. Infect. Dis. Model. 6, 751–765.

Dweck, E., et al., 2020. Impactos macroeconômicos e setoriais da Covid-19 no Brasil. Nota Técnica, IE-UFRJ.

Eichenbaum, M.S., Rebelo, S., Trabandt, M., 2021. The macroeconomics of epidemics. Rev. Financ. Stud. 34 (11), 5149–5187.

Eichenbaum, Martin S., Rebelo, S., Trabandt, M., 2020. The Macroeconomics of Epidemics. NBER Working Paper, No. 26882.

Farhi, E., Werning, I., 2020. Dealing with the Trilemma: Optimal Capital Controls with Fixed Exchange Rates. NBER Working Paper No. 18199.

Ferguson, N., Cummings, D., Fraser, C., Cajka, J., Cooley, P., Burke, D., 2006. Strategies for mitigating an influenza epidemic. Nature 442, 448–452.

Ferguson, N., et al., 2020. Impact of Non-pharmaceutical Interventions (NPIs) to Reduce COVID-19 Mortality and Healthcare Demand. Imperial College COVID-19 Response Team Report, No. 9.

Ferrari, T., Dusi, L., Lopes, D., Pompermayer, M., 2019. Estimativa do valor da vida estatística e do valor da economia de tempo em viagens nas rodovias brasileiras com a utilização de pesquisa de preferência declarada. Texto para Discussão IPEA No. 2533.

Fongaro, G., et al., 2021. The presence of SARS-CoV-2 RNA in human sewage in Santa Catarina, Brazil, November 2019. Sci. Total Environ. 778.

Góes, G.S., Borelli, L., 2021. Implicações da descoordenação entre as esferas federal e estadual na condução de políticas públicas de combate à pandemia da Covid-19 no Brasil. Cadernos ENAP No. 85.

Haddad, E., Perobelli, F., Araújo, I., 2020a. Input-Output Analysis of COVID-19: Methodology for Assessing the Impacts of Lockdown Measures, TD NEREUS 1–2020. USP.

Haddad, E., Perobelli, F., Araújo, I., Bugarin, K., 2020b. Structural propagation of pandemic shocks: an input–output analysis of the economic costs of COVID-19. Spat. Econ. Anal.

Hallal, P., et al., 2020. Remarkable variability in SARS-CoV-2 antibodies across Brazilian regions: nationwide serological household survey in 27 states. medRxiv. https://doi.org/10.1101/2020.05.30.20117531

Kermack, W., McKendrick, A., 1927. A contribution to the mathematical theory of epidemics. Proc. R. Soc. Lond. Ser. A 115 (772), 700–721.

Krueger, D., Uhlig, H., Xie, T., 2020. Macroeconomic dynamics and reallocation in an epidemic, NBER Working Paper, No. 27047.

Lee, B., Brown, S., Cooley, P., Zimmerman, R., Wheaton, W., Zimmer, S., Grefenstette, J., Assi, T.-M., Furphy, T., Wagener, D., 2010. A computer simulation of employee vaccination to mitigate an influenza epidemic. Am. J. Prev. Med. 38, 247–257.

Medeiros, M., Street, A., Valladão, D., Vasconcelos, G., Zilberman, E., 2020. Short-term COVID-19 Forecast for Latecomers. Departamento de Economia, PUC-Rio Texto para Discussão #670.

Mellan, T. et al., 2020, May. "Report 21: Estimating COVID-19 cases and reproduction number in Brazil", Imperial College COVID-19 Response Team.

Morato, M.M., Bastos, S.B., Cajueiro, D.O., Normey-Rico, J., 2020. An optimal predictive control strategy for COVID-19 (SARS-CoV-2) social distancing policies in Brazil. Annu. Rev. Control 50, 417–431.

Nunes, L., Rocha, R., Ulyssea, G., 2020. “Vulnerabilidades da População Brasileira à COVID-19: Desafios para a Flexibilização do Distanciamento Social”, Nota Técnica #9, IPES.
Rabelo, M., Soares, J., 2020, April. “The Macroeconomics of Epidemics: results for Brazil”, Draft.
Rache, B., Nunes, L., Rocha, R., Lago, M., Fraga, A., 2020. “Como conter a curva no Brasil? Onde a epidemiologia e a economia se encontram”, Nota Técnica #4, IPES.
Rocha, G., de Morais, R., Klug, L., 2019, October. “O custo econômico da poluição do ar: Estimativa de valor da vida estatística para o Brasil”, Texto para Discussão IPEA No. 2517.
Susskind, D., Vines, D., 2020. The economics of the COVID-19: an assessment. Oxf. Rev. Econ. Policy 36, S1–S13.
Viegas, M., et al., 2020. Os primeiros 80 dias da pandemia da COVID-19 em Belo Horizonte: da contenção à flexibilização. Nova Econ. 30, 701–737.